Precision Pointing in Space Using Arrays of Shape Memory Based Linear Actuators

by

Nikhil Sonawane

A Thesis Presented in Partial Fulfillment
of the Requirements for the Degree
Master of Science

Approved November 2016 by the
Graduate Supervisory Committee:

Jekanthan Thangavelautham
Huei-Ping Huang
Kiran Solanki

ARIZONA STATE UNIVERSITY

December 2016

ABSTRACT

Space systems such as communication satellites, earth observation satellites and telescope require accurate pointing to observe fixed targets over prolonged time. These systems typically use reaction wheels to slew the spacecraft and gimballing systems containing motors to achieve precise pointing. Motor based actuators have limited life as they contain moving parts that require lubrication in space. Alternate methods have utilized piezoelectric actuators. This paper presents Shape memory alloys (SMA) actuators for control of a deployable antenna placed on a satellite. The SMAs are operated as a series of distributed linear actuators. These distributed linear actuators are not prone to single point failures and although each individual actuator is imprecise due to hysteresis and temperature variation, the system as a whole achieves reliable results. The SMAs can be programmed to perform a series of periodic motion and operate as a mechanical guidance system that is not prone to damage from radiation or space weather. Efforts are focused on developing a system that can achieve 1 degree pointing accuracy at first, with an ultimate goal of achieving a few arc seconds accuracy. Bench top models of the actuator system has been developed and working towards testing the system under vacuum. A demonstration flight of the technology is planned aboard a CubeSat.

To my Parents Sunil Sonawane and Sunita Sonawane

ACKNOWLEDGMENTS

Firstly, I want to express gratitude to my Chair and Mentor Dr. Jekan Thanga for his guidance, support and motivation. His constant encouragement has helped me explore a facet of engineering I wouldn't have explored otherwise. This has helped me grow as an engineer and as a person.

I would like to thank my Dr. Huei Ping Huang and Dr. Kiran Solanki who have agreed to be on my committee and provided me with the right information at the right time. I would also like to acknowledge efforts made by Karan Sautabine from Dynalloy, Inc. who has constantly been a source of motivation and provided all the technical help required at several stages while completing the thesis work.

In the end I would like to thank my colleagues and fellow students at the SpaceTREx Lab at ASU, Aman Chandra for constant help and support for helping me proof read my thesis document, Andrew Warren for his help setting up electronics for my experiments, Laksh Raura and Salil Rabade for their valuable inputs and interests in the project.

TABLE OF CONTENTS

Page

LIST OF TABLES

Table Page

LIST OF FIGURES

Figure Page

Figure Page

Figure Page

Figure Page

CHAPTER 1

INTRODUCTION

The evolution of space programs has made it necessary to envision new missions related to exploration and discovery. Astrophysicists along with public are excited by deep space pictures from Hubble telescope. Facts about neighboring solar systems, changing atmosphere of Earth can be explored if observed from space itself. Thus, the focus of research is in alignment towards developing spacecraft and instruments to support these deep space missions [1].

Deep space exploration as a focus area deals with the exploration of deep space, within or away from the Solar System involved with exploring the distant regions of outer space. [2] Physical exploration of space is conducted both by human spaceflights (deep-space astronautics) and by robotic spacecraft. As we go deep into space, the surface area of the space structures increases in size as the power requirements, the communication precision increases with increasing distance. For example, in case of antennas, the gain is given by the formula –

$$G_{\max} = 4\pi\eta A f^2 / c^2 \qquad [3]$$

For the same amount of gain, as the spacecraft moves away from the earth, the size of the antenna increases. Thus increasing the cost of the mission.

The Deep Space Network is NASA's international array of giant radio antennas that supports interplanetary spacecraft missions, plus a few that orbit Earth. The DSN also provides radar and radio astronomy observations that improve our understanding of the solar system and the larger universe. The antennas of the Deep Space Network are the indispensable link to explorers venturing beyond Earth. They provide the crucial

connection for commanding our spacecraft and receiving their never before seen images and scientific information on Earth, propelling our understanding of the universe, our solar system and ultimately, our place within it. [4] Deep Space Communications Complexes, have 70-meter antenna as shown –

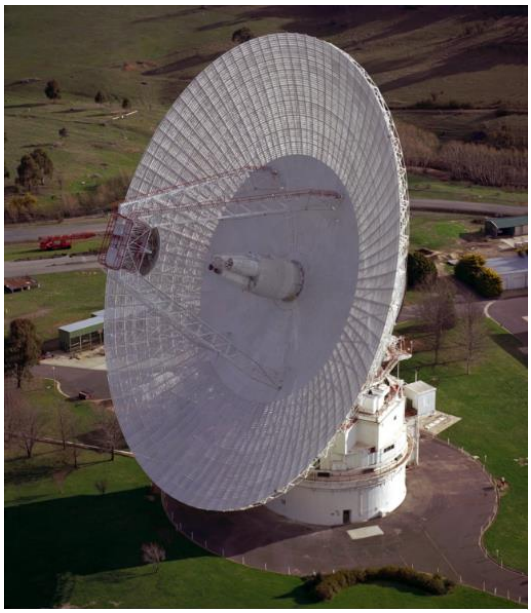

Figure 1 - View of Canberra
Communication Complex [4]

One of the major ways to cut down costs is to develop cost effective mechanical systems to handle such large structures - the platforms upon which many missions depend. While focus has been on large in-space "truss" platforms for large mirrors and telescopes, the need has shifted to developing smaller, more affordable and higher precision structures designed for deep-space missions. [1]

The study of structural responses, new mechanisms and components will naturally lead to the need for new, advanced materials. New materials must meet several criteria [1]:

- Dimensional Stability. A dimensionally stable material retains its size and shape with changes in temperature. This is especially important in a spacecraft or structure which may orbit Earth, moving in and out of the sun's heat.
- Light Weight. It takes ten pounds of resources to get one pound into space and back. Therefore, the lighter the material, the less costly it is to the mission.
- Environmental Stability and Durability. Most components must be durable in the harsh space environment, which includes radiation, atomic oxygen and a vacuum.
- Strength/Stiffness. How much load a material can hold before breaking and how flexible it is, are two different considerations determined by the desired application.
- Manufacturability. A material that is hazardous to the people who are manufacturing it or to the environment can be more expensive to make because of the special requirements to handle and dispose of it.
- Cost Effectiveness. The cost of a material, including production and testing, is a major consideration and can be the determining factor in whether or not it is used.

Considering communications as the focus and introduction of new materials for deep space missions, developing of a low cost, easy in construction, cost effective and heavy load bearing antenna pointing mechanism actuated by these materials is the objective of work mentioned in this thesis.

1.1 Background

1.1.1 Pointing Mechanisms for Space Application

A key component of any practical, covert laser communications system will be the pointing and tracking mechanism. Such a system requires a mechanism that is (1) easily manufacturable therefore inexpensive; and which has (2) high slew rates; (3) high accuracy; and (4) wide, singularity-free range of acquisition. [5]

For the antennas, the advantage of pointing the antenna individually facilitates the pointing of the solar panels independently towards the sun and also maintain communication with the ground station simultaneously.

The pointing mechanisms in space can be used for the following applications –

- Pointing of space craft antennas
- Pointing of solar panels
- Pointing of optical terminals
- In-orbit adjustment or alignment of equipment. [6] [7]

Traditional pointing mechanisms for small satellites use 3 axis reaction/ momentum wheels to facilitate angular movement depending on requirements. The larger satellites and spacecraft's have thrusters to provide directional control for positioning and attitude control. Thrusters are chemical propulsion systems which can be monopropellant. Single fluid or bipropellant i.e. double liquid type. The latest advancements have led to the use of higher energy electric propulsion systems and ion acceleration based thrusters.

In case of satellites comparatively bigger in size, pointing solutions are generalized to two-phase system, a gimbal or a universal joint for position. The current antenna pointing mechanisms for the bigger satellites are generally based on varying degrees of accuracy. Commonly used pointing mechanisms may be classified as:

1. Single Axis

These antenna pointing systems are based on rotation about single axis. They typically consist of following components

1. Ball bearing pair
2. An optical encoder
3. A torque motor
4. An electric cable winding to establish connections between fixed and rotating parts [8]

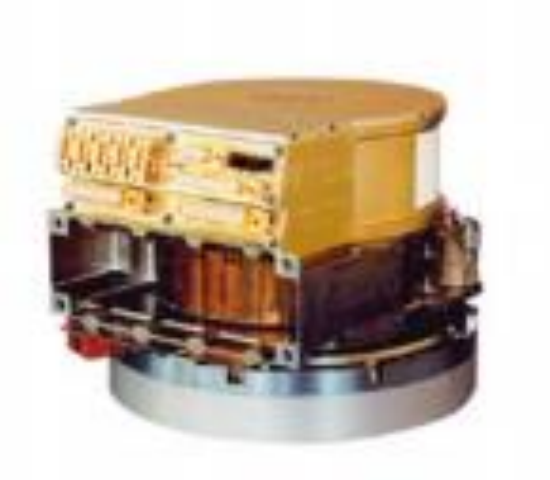

Figure 2 - Single Axis APM (SILEX) [8]

b. Two-Axis

The APM (Antenna Pointing Mechanisms) are typically two-axis gimbals. Each rotation axis comprises a hybrid stepper motor, spur gear transmission, and magnetic encoder. A spiral wrap DC harness passes the motor and telemetry channels through the azimuth axis to the elevation axis, while RF non-contact rotary joints are used to pass the RF feed through each axis. Antenna motion relative to the spacecraft is produced in either an elevation-over-azimuth or a cross-axis format. The elation-over-azimuth format can yield full hemispherical coverage, while the cross-axis format is useful for producing defined angular motion in spacecraft coordinates. The wide variety of antenna positioner

assembles are compact, two-axis gimbals which are ideal for supporting and positioning small- to medium- to large-sized spacecraft communications antennas [9]. Gimbals can be configured with either azimuth-elevation or X-Y (crossed axis) geometry,

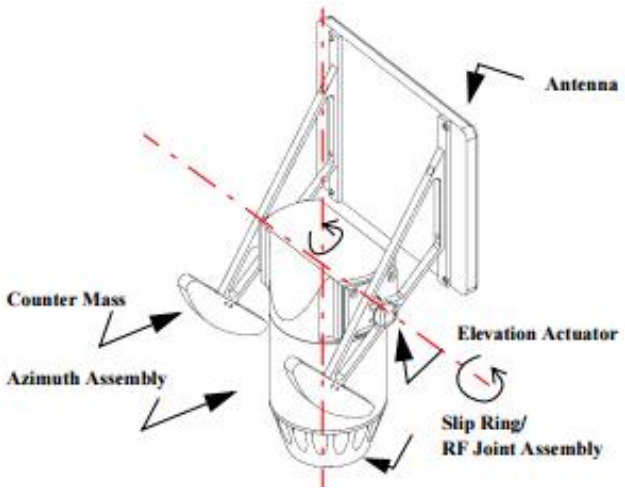

Figure 3 - 2-Axis APM [10]

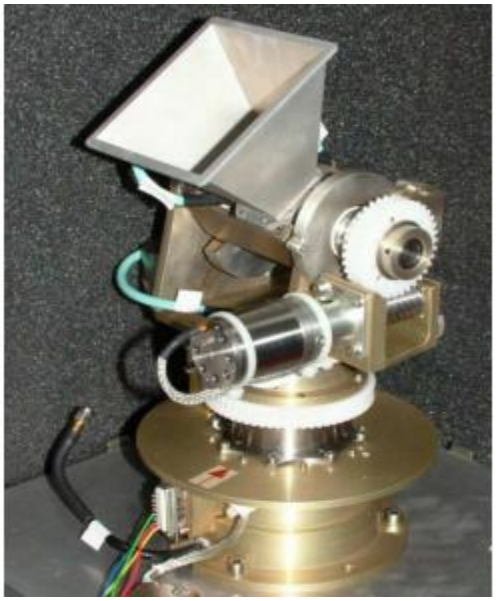

Figure 4 - Azimuth-Elevation Engineering Model APM [11]

Few drawbacks of these systems include slowed response time, limitation on the motion range an also due to singularities pertaining to system used.

1.1.2 Introduction to shape memory alloys

Smart materials have become a suitable choice for various engineering applications due to their inheritance of special properties. The general feature of all of them is the fact that one or more properties might be significantly altered under controlled condition. These include piezoelectric materials, magneto-rheostatic materials, electro-rheostatic materials, and shape memory alloys. Among these the special property possessed by the Shape memory alloys is having the tendency to return to its original memorized form on application of heat to increase it over its transformation temperature. [12]

The effects exist in shape memory alloys due to their macroscopic properties. There exist two stable phases, the transition between which gives rise to the effect. The shape memory alloys exist in the form of Martensite at low temperature and Austenite at high temperature. The Martensite additionally can be in two forms: twinned and detwinned. A phase transformation which occurs between these two phases upon heating/cooling is the basis for the unique properties of the SMAs. The key effects of SMAs associated with the phase transformation are *pseudoelasticity* and *shape memory effect*. [13]

1.1.2.1 Shape Memory Effect

If mechanical load is applied to the material in the state of twinned martensite (at low temperature) it is possible to detwin the martensite. Upon releasing of the load, the material remains deformed. A subsequent heating of the material to a temperature above A^{0f} will result in reverse phase transformation (martensite to austenite) and will lead to complete shape recovery, as shown in Figure (5). The below described process results in manifestation of the *Shape Memory Effect* (SME).

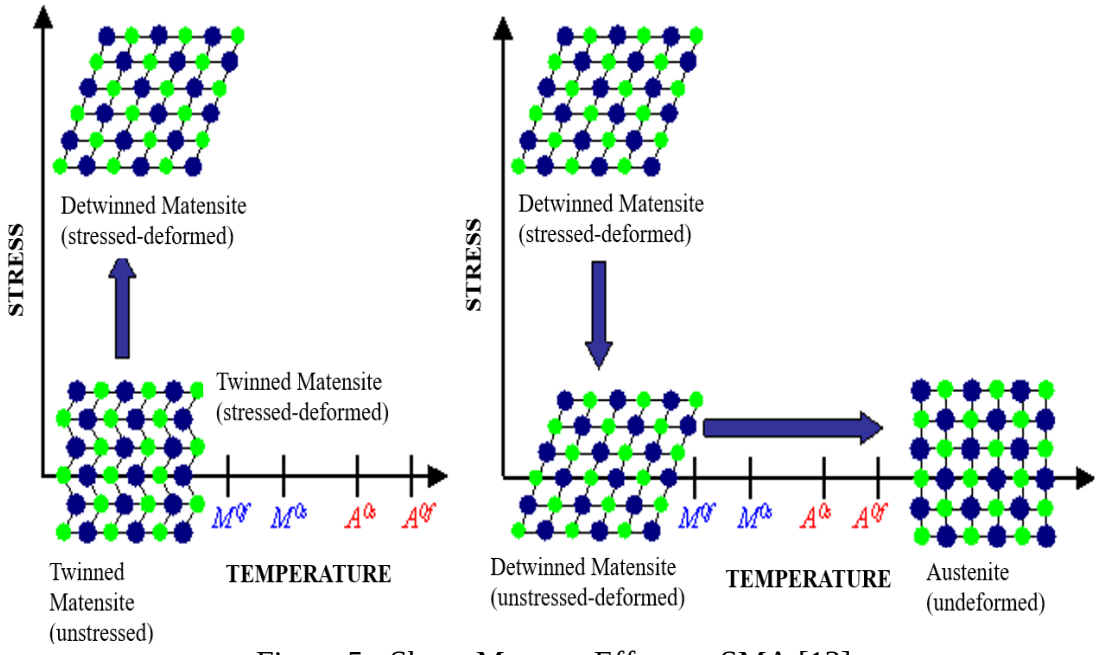

Figure 5 - Shape Memory Effect on SMA [13]

It is also possible to induce a martensitic transformation which would lead directly to detwinned martensite. If load is applied in the austenitic phase and the material is cooled, the phase transformation will result in detwinned martensite. Thus, very large strains (on the order of 5-8%) will be observed. Reheating the material will result in complete shape recovery.

1.1.2.2 PseudoElastic Behavior

It is also possible to induce a phase transformation by applying a pure mechanical load. The result of this load application is fully detwinned martensite with very large strains observed. If the temperature of the material is above A0f, a complete shape recovery is observed upon unloading, thus, the material behavior resembles elasticity. Thus the above-described effect is known under the name of Pseudoelastic Effect. A loading path

demonstrating the pseudoelastic effect is schematically shown in Figure (6), while the resulting stress-strain diagram is shown in Figure (7)

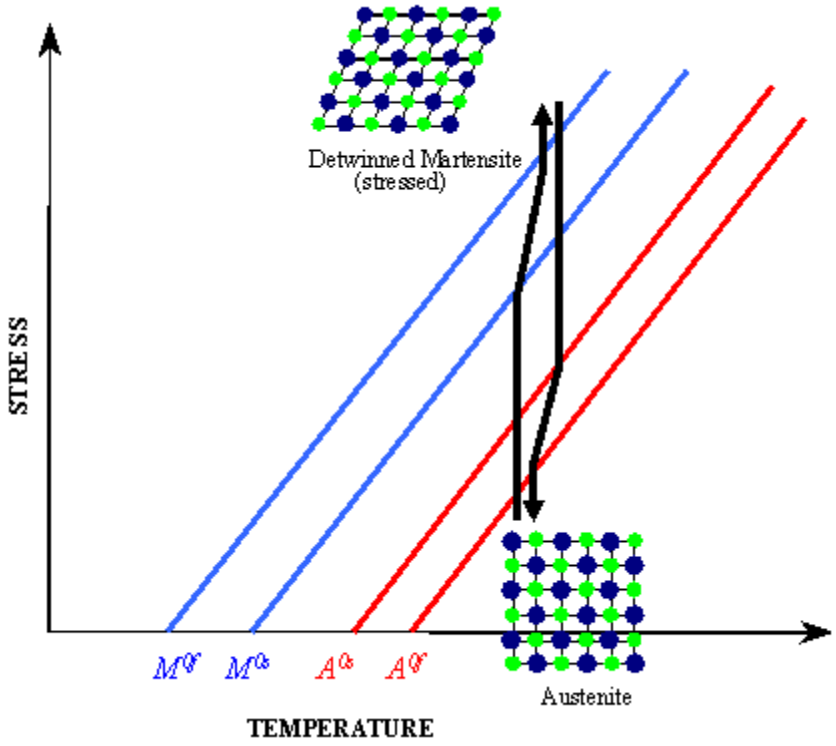

Figure 6- Pseudoelastic Loading Path [13]

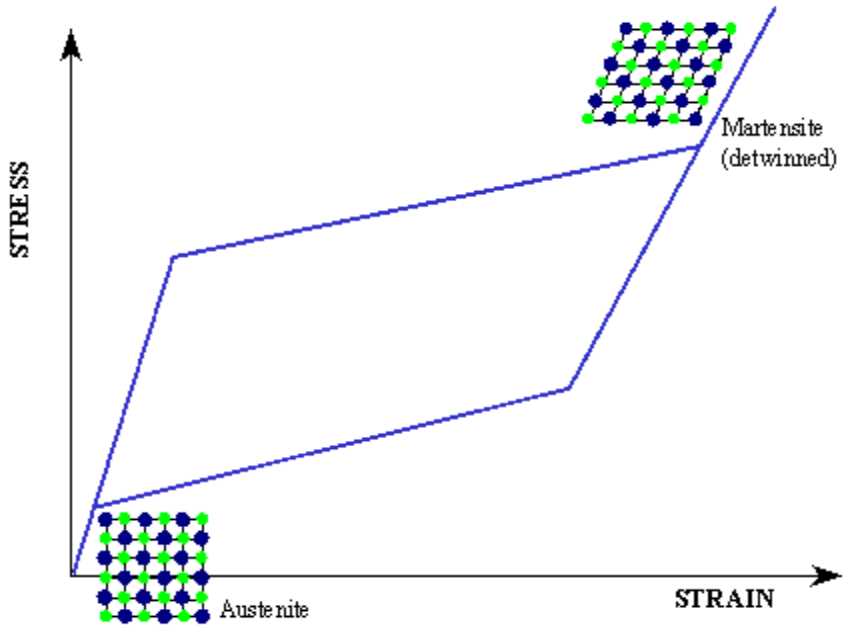

Figure 7 - Pseudoelastic stress-strain diagram [13]

1.2 Motivation

There are various applications of SMA's among which few are [14] -

1. eye glass frames
2. couplings
3. rivets
4. clamps
5. Vibration dampers
6. Vascular stents
7. Active/Passive actuators

For our application we focus on the actuation capabilities of SMA's due to their unique property of returning to its original shape after large strains. SMA's have the ability of providing significant amount of actuation with a smaller volume of space. For Small satellites application, when compared to other actuators having stringent space constraints

make the use of SMA's ideal. The SMA's have the best efficiency in terms of Specific Work Output when compared to all the commercially used micro actuators, as seen from the graph.

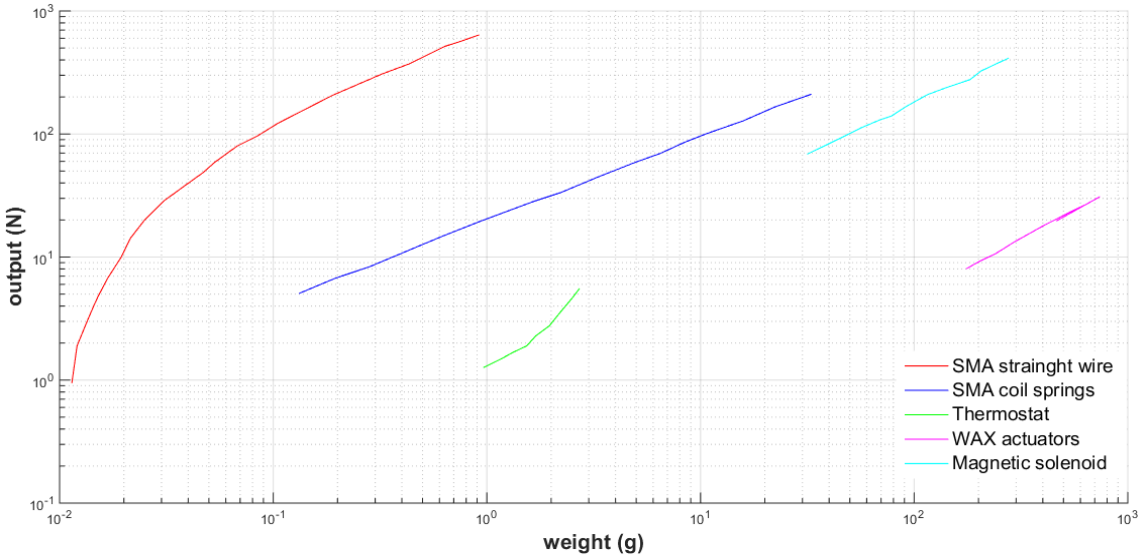

Figure 8 - Specific work output of different micro actuators [15]

Other advantages of using SMAs are they have high load bearing capacity for a given size, SMA wires can exert as much as 600 million N/m^2 (Dynalloy,Inc.) [18]. The SMA's have the tendency to contract on heating and thus provide a source of actuation. Further the SMA's can be used in any axis to provide the system with multiple degrees of freedom, which increases the flexibility of motion and making it constraint free.

The application of SMA to antenna has the potential of enabling low transmitter power consumption and reduced ground-station dish size for comparable data rates as conventional antenna.

1.3 Problem Statement

In order to develop a pointing mechanism for antenna using shape memory alloy, we set out to demonstrate an SMA based linear actuator which would involve design,

constructing and testing a lab scale model which would obtain precise pointing to 1-degree accuracy along freedom to move in any direction. The design of the system was done keeping the following factors in mind:

1. Precision requirements

SMA's used for actuation purpose depends on various factors like stress levels, strain levels, the surrounding temperature and type of application which hampers their precision in exact amounts of actuation requirements.

2. SMA Temperature Control

SMA's are basically resistors which change phase when specific value of transformation temperature is reached. There are two major ways to increase their temperature

a. By direct Heating
b. By providing current

The temperature developed in an SMA cannot be controlled by direct heat and thus their use for passively actuated systems is limited and depends on their transition temperatures However, a calculated value of current based on factors like diameter of wire, transition temperature can be used for better actuation results.

3. Hysteresis

The figure (9) shows a typical stress-free temperature-induced martensitic transformation and its inverse transformation under a temperature excitation cycle.

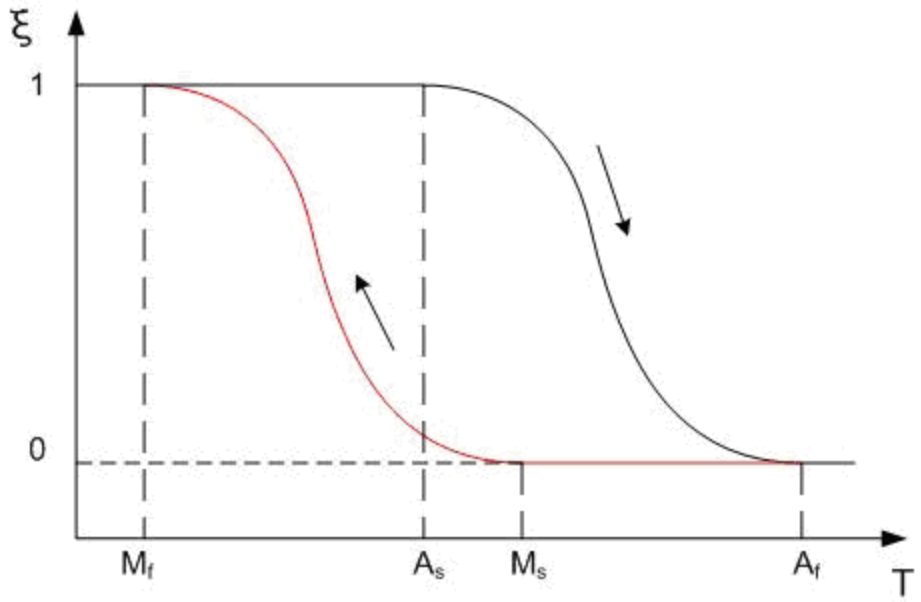

Figure 9- Hysteresis Loop for Shape Memory effect shown by SMA [16]

Four transition temperatures characterize the transformation loop: Martensite start temperature (Ms), Martensite finish temperature (Mf), Austenite start temperature (As) and Austenite finish temperature (Af). These critical temperatures pinpoint the beginning and the end of the forward (Martensite) and the inverse transformation. It is noticeable that the temperature-deformation loop is hysteretic due to internal phase friction.

4. Strain rates control

The amount of force to strain the SMA structures is limited. Since over straining has adverse effects on the properties of the SMA and the number of cycles they can sustain reduces drastically. The maximum strain to which SMA's can operate for millions of cycles in 3-4 %. This values limits the high strain causing applications for SMA's like folding them multiple times within the CubeSat structure limiting the optimum use of stowage available.

1.4 Objective

The objective is to implement the use of SMA's for antenna pointing system so as to achieve low cost, and reliable actuation technology.

The work towards this thesis is intended to demonstrate the following:

1. Demonstrate lab scale linear actuation using the contraction of SMA structures.
2. Demonstrate SMA based pointing mechanism on lab scale.
3. Demonstrate latching (or harnessing) mechanism using SMA on lab scale to attain a pre-determined level of accuracy.
4. Propose a system level concept design for implementation on CubeSats.

CHAPTER 2

LITERATURE REVIEW

2.1 Antenna Pointing Mechanisms

Most of the space missions necessitate the use of accurate pointing mechanisms for the antennas, optical terminals, pay loads, solar panels etc. for successful operation. These mechanisms are characterized by their ability to provide precision movement at low power consumption and high reliability. [6]

Following are accuracy requirements for pointing mechanisms in various applications.

1. high gain antennas – fraction(s) of a degree
2. inter-satellite optical links – micro-radians
3. instrument optical delay lines – Nano-radians [6]

Optimization of the antenna pointing mechanisms depend on accuracy requirements requires for enhance mechanization performance and reduction in system cost and mass.

2.1.1 Common Pointing Mechanisms

PM's are selected on basis of their size and the type of entity used for this application. The different mechanisms are based on concepts dealing with axis of rotation i.e. real or virtual, the mechanics for pivot point, type of motor being used, drive mechanism for motor and resolver [17].

2.1.2 Mechanism concepts for Antenna Pointing:

1. Gimbal-Based Antenna Pointing Mechanism Concepts

   These mechanisms generally use ball bearing along with stepper or DC motors about each axis depending if its single axis or double axis based. The advantage of

this mechanization is to allow large angle deflection for the antennas, but the total mass consideration is also an important aspect to be taken care of.

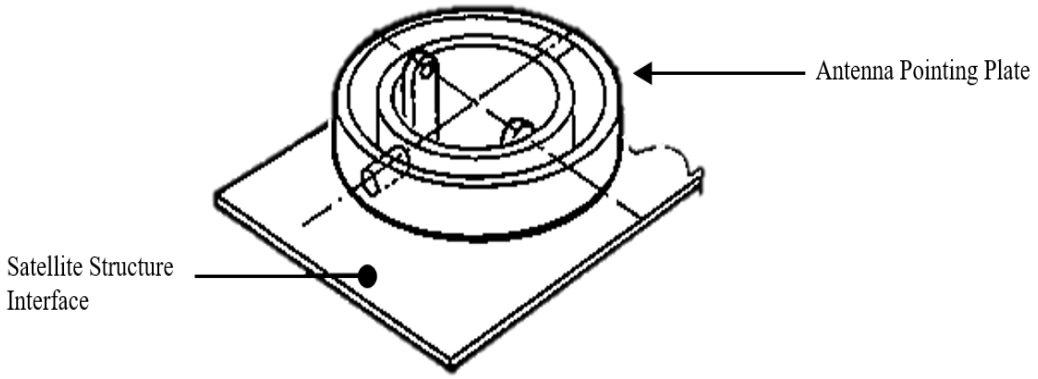

Figure 10- Principle of APM using Gimbals [17]

Commercially, this type of mechanism is used extensively. Some examples are SSTL APM, NEA's P3[5] [18][19]

2. Pivot-Based Antenna Pointing Mechanism Concepts

These mechanisms are derived from previous work on gimballed momentum wheels, the one shown in the figure (11) uses the screw jack and stepper motor mechanization which features full redundancy through symmetrical actuator and pivot arrangements. Screw jack mechanisms are replaced with linear DC motors featuring no contact between movable pieces but requiring caging for launch.

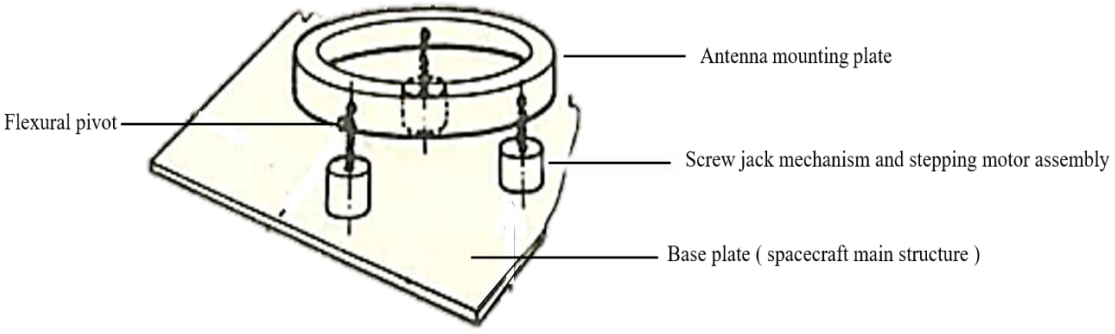

Figure 11 - Principle of Pivot-Based APM [17]

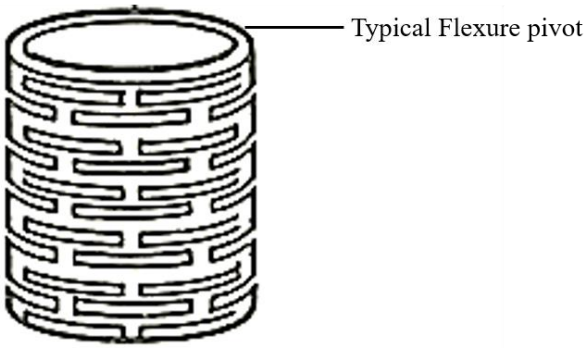

Figure 12 - Flexural pivot [17]

3. This particular type is an extension to the first type, where an additional gimbal is used to provide a virtual axis of rotation to antenna which differs from the existing physical gimbal axis by a certain distance. The calculations are based on the selection of the blade stiffness as per figure (13) –

$$d3 = 2d1 \quad and \; d1 = \frac{\theta 2}{2\theta 1} d2$$

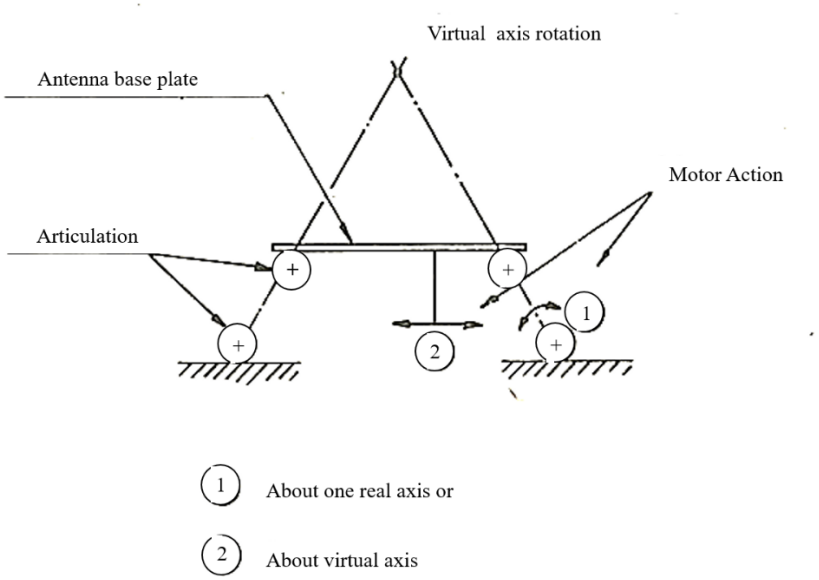

Figure 13 - Principle of a one-axis APM providing rotation about virtual axis (for small angle only <3 degrees) [17]

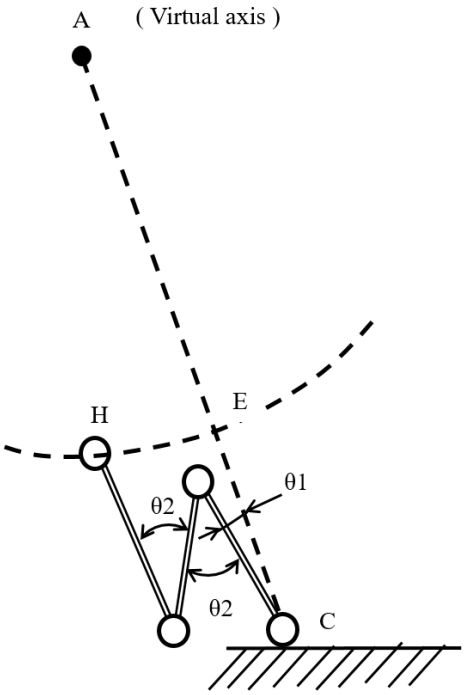

Figure 14 - Principle of articulation for rotation about virtual point [17]

In figure (14),

AH = constant at 2nd order requires:

$$\frac{\theta 2}{\theta 1} = \frac{1 + d + \sqrt{2l(l+d)}}{1 - d}$$

Notations –

AE = l

CE = d

The applicability of these concepts are viable in two conditions –

a. When the PM orients only the antenna reflector, rotations can be performed around the antenna horn and the antenna focalization can be maintained within a few degrees, whatever the beam rotation may be.

b. When the PM orients the whole antenna, the rotations can be performed around the satellite center of mass and dynamical decoupling between antenna and satellite main body can be optimized according to the satellite configurations.

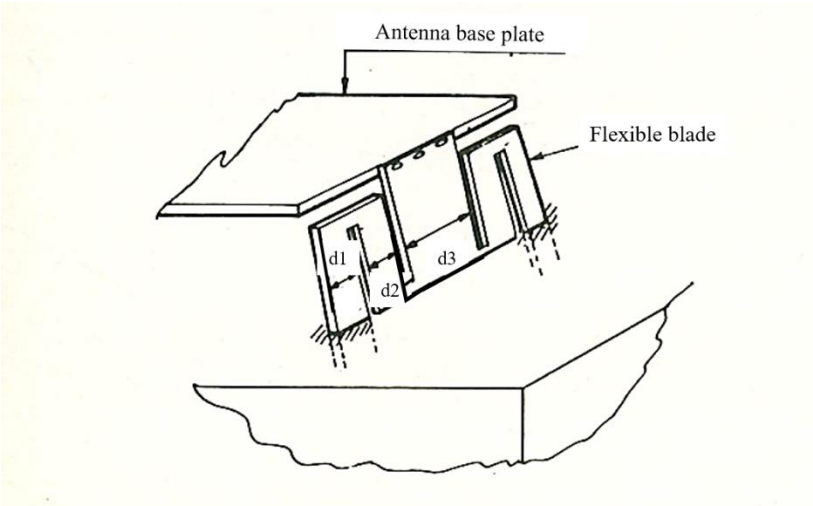

Figure 15- Flexible blade shaped to generate multiple equivalent rotation axis. Rotation about virtual axis is obtained for angles up to 10 to 15 degrees [17]

4. This type is based on 3 rotation axes biased to each other, which are placed such that their motion is in the form of a cone to provide control to the antenna for pointing. The 3 axis are required to make corrections with regards to azimuth and elevation angles. Using this particular type very high stiffness and accuracy of the order of 0.005 degrees or less can be obtained.

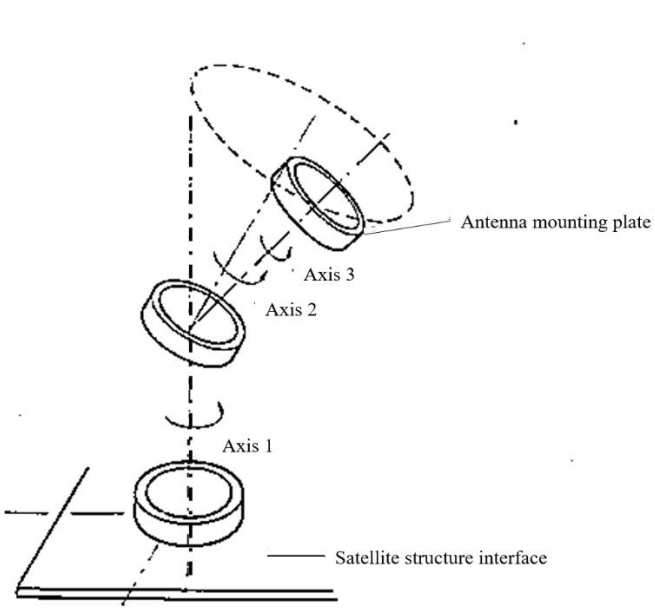

Figure 16 - APM type 4 [17]

2.2 SMA Applications

To use SMA's in pointing mechanisms, their feasibility in existing mechanisms needs to be evaluated. The following SMA characteristics are of interest:

1. Shape Memory Effect

2. Super elasticity

The dynamic behavior of SMA's can be characterized by the following functions: [16]

a. Free recovery - This function identifies SMA's as displacement causing elements with no work produced. Applications include control devices, relay mechanisms.

b. Constrained Recovery – Large stress is developed as this function averts the movement of the SMA. Applications are fittings, couplings and connectors for machinery.

c. Actuator – SMA's are widely used as actuators, the function being applying force to cause a displacement and perform some amount of work. Applications include for latching actuator, small displacement linear actuators, rotary actuators.

d. Superelasticity – This function facilitates the SMA structure to restore its shape even after large elastic strains. Applications include use in glass frames.

e. High damping capacity – This particular function uses the combination of super elasticity and damping to enhance specific applications. Applications exist for gold industries in golf club inserts. A proprietary, high-damping shape memory alloy called Zeemet® has been developed by Memry specifically for the golf industry. The elastic property keeps the ball on the club face longer. That supplies more spin to the ball but not at the expense of distance [16].

2.2.1 Actuation using SMA

Among all the above functions, the actuation functions find its application for space in the most effective way. The SMA's actuation abilities provide the motivation to do further research regarding existing mechanisms used, and its scope for further analysis.

In wire form, Nitinol uses the shape memory effect to convert thermal energy into mechanical energy in the form of a linear contraction. To accomplish this, a longitudinal force is first applied to the Nitinol wire in the martensite phase to induce an initial

longitudinal deformation. Then, when the Nitinol is heated through the transformation temperature the strain recovery generates a contracting force. Because linear contraction is useful in many different applications, this is the form in which it is typically produced on large scale and sold at relatively low cost. The Nitinol wire used in this thesis is produced by Dynalloy Inc., and sold under the trade name Flexinol in a variety of diameters and transition temperatures [20].

The movement or stroke of the actuator (muscle wire) is measured as a percentage of the length of the wire being used and is determined, in part, by the level of stress one uses to reset the wire, or to stretch it in its low temperature phase. This opposing force, used to stretch the wire, is called the bias force. In most applications, the bias force is exerted on the wire constantly, and on each cycle as the wire cools, this force elongates it. If no force is exerted as the wire cools, very little deformation or stretch occurs in the cool, room temperature state and correspondingly very little contraction occurs upon heating. Up to a point the higher the load the higher the stroke. The strength of the wire, its pulling force and the bias force needed to stretch the wire back out are a function of the wire size or cross sectional area and can be measured in pounds per square inch or "psi".

If a load of 5,000 psi (34.5 MPa) is maintained during cooling, then about 3% memory strain will be obtained. At 10,000 psi (69 MPa), about 4% occurs, and with 15,000 psi (103 MPa) and above, nearly 5% is obtained. However, there is a limit to how much stress can be applied. Far more important to stroke is how the wire is physically attached and made to operate. Dynamics in applied stress and leverage also vary how much the actuator wires move. While normal bias springs that increase their force as the actuators contract have only 3-4% stroke, reverse bias forces which decrease as the actuator wires

contract can readily allow the wire to flex up to 7%. Mechanics of the device in which it is used can convert this small stroke into movements over 100% of the wires' length and at the same time provide a reverse bias force. [20]

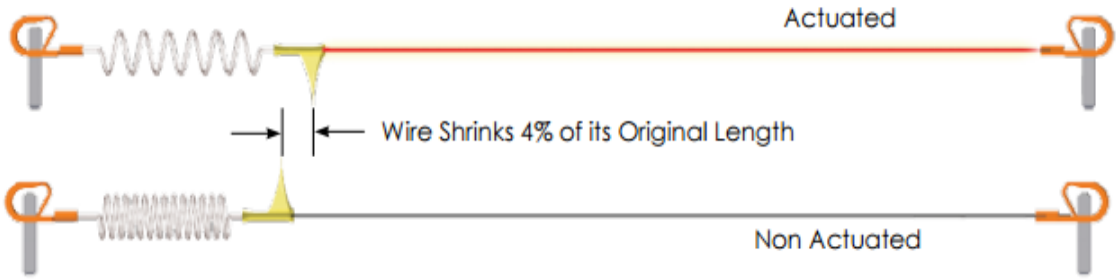

Figure 17- Actuation of a SMA wire

2.2.2.1 Limitations on the force –

The force that the actuator wire can exert when heated is limited by the strength of the high temperature austenitic phase. The phase transformation, or crystal change, that causes the memory effect has more driving force than the strength of the parent material, so one must use care not to exceed that yield strength. The yield strength of actuator high temperature phase is over 50,000 psi (345 MPa), and on a single pull the wire can exert this force. To have repeat cycling, however, one should use no more than 2/3 of this level, and forces of 20,000 psi (138 MPa) or below give the best repeat cycling with minimal permanent deformation of the wire [20]

2.2.2 Applications of SMA's for Linear Actuation and Load Bearing Mechanisms –

1. Large force shape memory alloy linear actuator [16]

This work involved developing a large force linear actuator using a set of SMA wires to pull 45359.2 grams force and provide a deflection of 0.8 inches. The given figure (18) shows the experimental setup

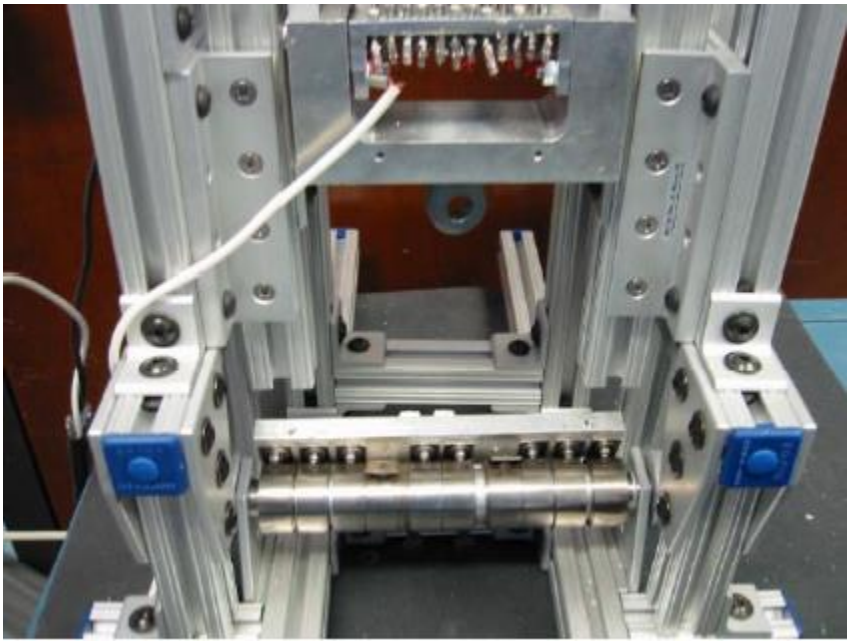

Figure 18 - Experimental setup [16]

2. MigaOneTM Linear actuator [22]

The MigaOneTM is a very thin electric actuator powered by Shape Memory Alloy (SMA) wires, providing a constant-force stroke of 0.375” generating a force of 11 N. The MigaOne has an end-of-stroke limit switch that prevents overheating of the SMA wires.

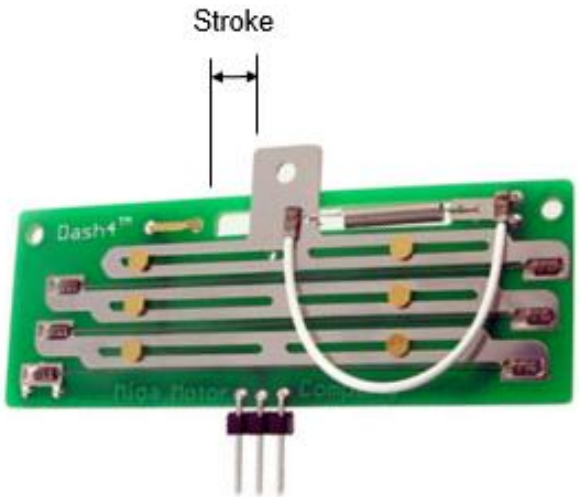

Figure 19 - Linear Actuator showing the range of stroke [22]

3. Solar Paddle Actuator for Small Satellites Using SMA [23]

This work was done towards developing a mechanism to point the Solar Paddles on a small satellite by 360-degree rotation. It uses 6 SMA springs and their linear actuation abilities are used for rotary motion using pulleys. The force generated for the system is 10 N. The shortcomings were usability for only 1000 cycles and rotation in one degree of freedom.

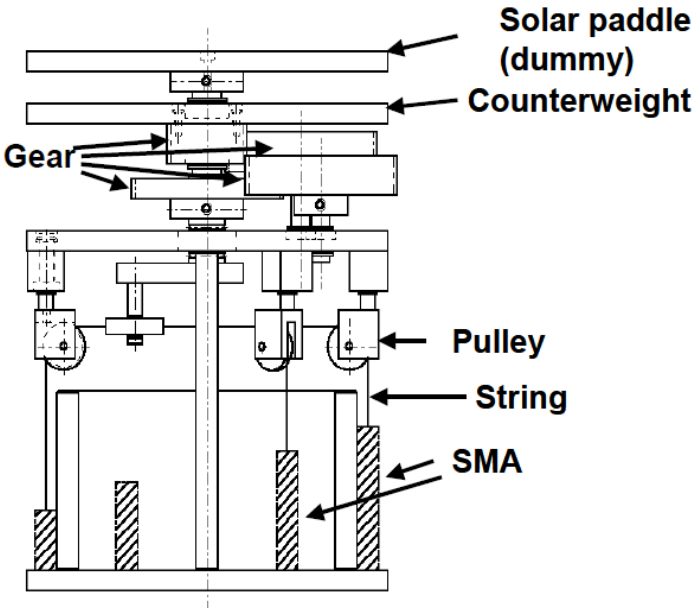

Figure 20 - Solar Paddle Actuator [23]

4. Design of a Shape Memory Alloy Actuated Compliant Smart Structure [24]

This is a spatial mechanism designed for large displacement. It incorporates nitinol pipe as the compliant structural member which in turn is actuated by a set of three SMA wires demonstrating both the shape memory effect as well as super elasticity properties. The SMA wires tend to provide elastic deformation, tilting the central structure. This mechanism has potential applications for endoscopic tip, micro mirror and antenna positioning devices, or as a general spatial compliant manipulator [24].

2.3 Latching Mechanisms using SMA's

The ability of the SMA's as a result of its shape memory effect has shown its ability to produce large forces in small amounts of time with small deflection. These properties have been successfully tested for latching mechanisms.

To develop antenna based pointing mechanism, the aim is to achieve highest degree of accuracy possible with minimum step size. The general use of stepper motors, or rotary actuators which may cause single point failure has been a concern. Therefore, experimental implementation of latching mechanism and its feasibility will be studied.

Pictorial presentation of basic latching mechanism is shown in given figure (21, 22)

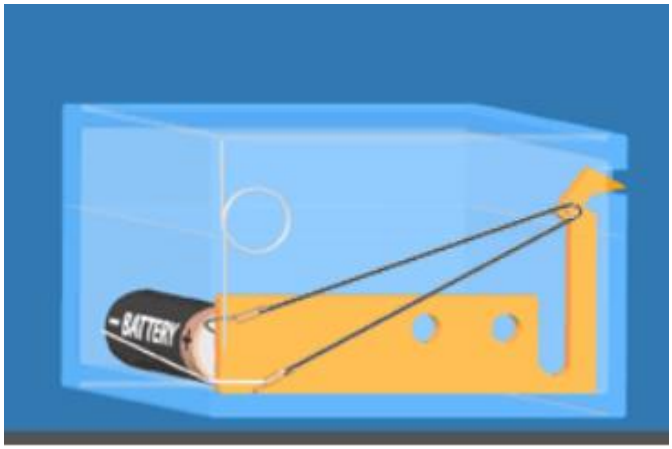

Figure 21 - The SMA wire in deactivated position. (Extended position)

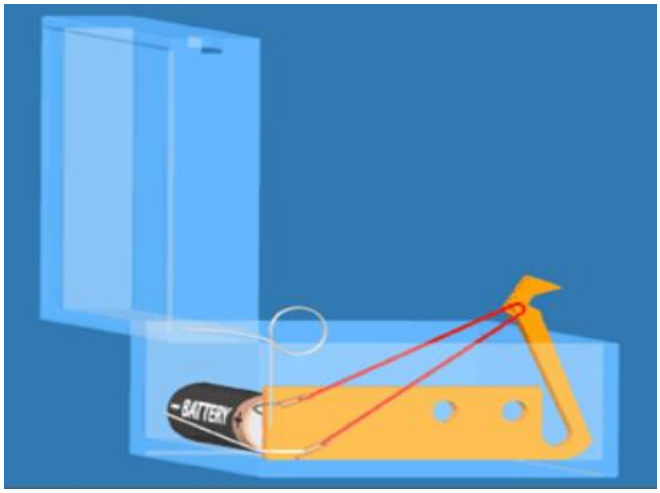

Figure 22 - The SMA wire in activated position. (Contracted position)

The existing latching mechanisms include -

1. Latching Actuator by AutoSplice [25]

The actuator develops a force of 50 grams for latching with a stroke of 3mm. The power required to achieve the stroke in one direction is 0.28 watt-seconds.

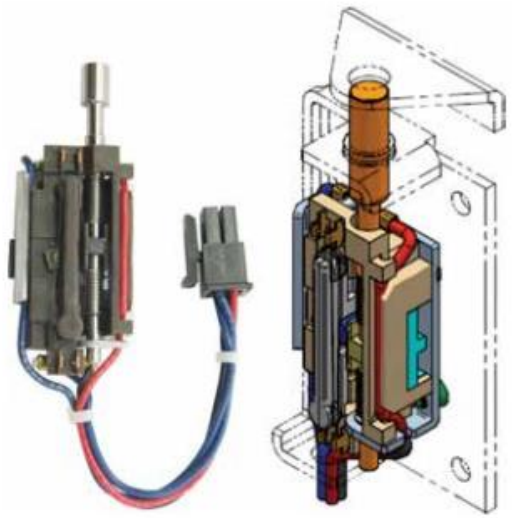

Figure 23 - Latching Actuator from AutoSplice [25]

2. Frangibolt™ separation system by TiNi alloy

The frangibolt is basically a nut and bolt assembly. It consists of a SMA cylindrical body with an integrated heater. The cylinder is notched to a bolt which in turn is attached to a nut or payload to be released. When current is passed through, the heater heats the cylinder body and fractures the bolt, this separates the nut bolt assembly and release of payload is achieved. The payload can be up to 20,000 lbf. [27]

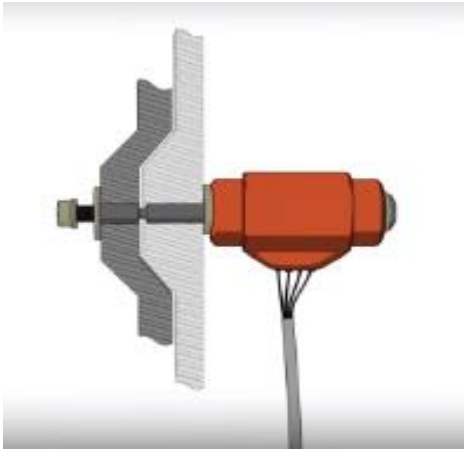

Figure 24 - Frangibolt initial configuration [27]

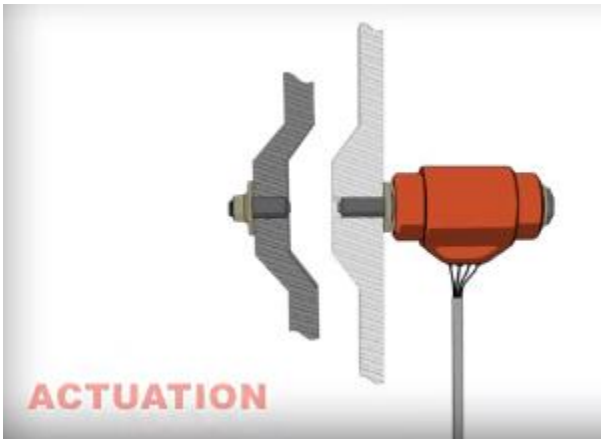

Figure 25- Frangibolt final configuration (activated) [27]

3. Pin puller

Pin Puller actuators are low-shock non-explosive SMA based mechanical devices in which a pressure cartridge causes a pin or piston to retract inside the structure frame, usually against a side load. In the extended position, the pin or output shaft can be seen to be loaded by a compression spring. The pin remains firmly locked in this position due a mechanical components block stroke [26].

Once actuated however, the actuator drives specific mechanical components releasing stroke and allowing the pin to retract under the force of the drive spring. The actuator is reset by manually moving the pin back into the extended position. The payload ranges from 5 to 1000 lbs. [26]

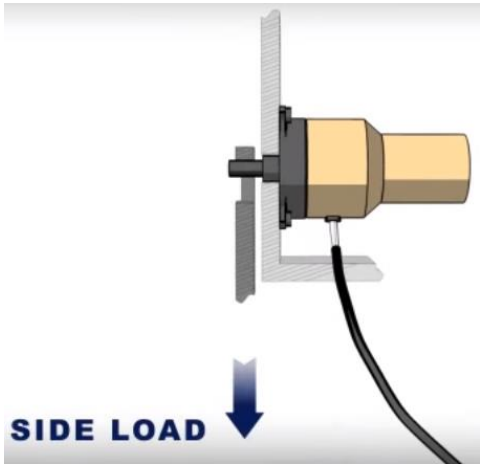

Figure 26 - Pinpuller initial configuration [26]

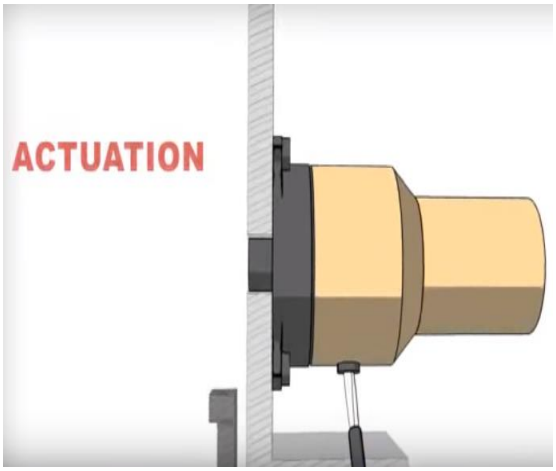

Figure 27 - Pinpuller final configuration. (activated) [26]

The various concepts for different configuration of antenna pointing mechanism provide design schemes for the proposed antenna pointing mechanism. The pivot based antenna pointing mechanism was decided to be most relevant to the applicability for the use of

SMA’s as it uses linear actuation of the screw jack mechanism. This linear actuation can be driven by SMA based linear actuators to serve the purpose.

The pre-existing applications of the SMA’s for linear actuation and latching gives an insight into the applicability of the use of SMA’s for obtaining a consistent stroke for large amount of cycles. It also helps setting design considerations for avoiding over straining and over stressing the SMA wire. This literature review helps in understanding the SMA behavior for different applications and also their relevant applicability for antenna pointing mechanisms.

CHAPTER 3

METHODOLOGY

To meet the objectives of the proposed system, a thorough methodology was adopted. This section deals with the methods to design the prototype for experimentation. The sections discussing the selection of materials and the shape configuration, the characterization of the SMA behavior, the selection of the mechanism to convert the small stroke from SMA to a useful magnified stroke, setting up the design parameters for the proper working of prototype mechanism without over straining / over stressing the SMA, analyzing the strength of multiple wires in parallel and final prototype design have been included within scope of this chapter.

The major subsystems for the antenna pointing mechanism assembly are the SMA based linear actuation assembly and the SMA based latching mechanism, thus to experimentally demonstrate a working SMA based pointing mechanism, work was conducted in following phases:

1. Demonstration of SMA actuation capabilities.

In order to understand the dynamic behavior of the SMA wires, we performed a number of experiments in the laboratory. Commercially available SMA's are generally drawn into wires or springs. In order to choose between the two, experiments were performed on both to understand their respective behaviors. Analysis of results reveled wires to be a more viable option.

2. Mechanism for latching SMA actuated components.

The latching mechanism would be used to control the motion of the linear actuation obtained with precision. The movement of the linear actuator takes place at a certain speed,

therefore the selection of the wire/spring was chosen based on fastest cycle times so that the latching can be done as per our position/angle requirements.

3.1 Material Selection

Design configurations incorporating spring and wires for the experimental phases described above are based on the following justifications:

1. In order to support large and heavy objects in space using SMA's, they would require to be efficient sources of momentum transfer. Hence, for the purpose of linear actuation, an initial design of the system was done using a wire/spring that could provide the maximum pulling force capacity. A study of the available wires revealed their pulling force to be proportional to their diameters. Wires of diameters 0.015 in and 0.020 having pulling capacities of 2250 grams and 3560 grams respectively were chosen for experimentation. Similarly, for the spring, a 0.020 inch diameter having highest pulling capacity of 243.3 grams was selected [20].

For the latching mechanism the wires with lowest cycle times and considerable force pulling capacity were chose. The diameters of the wires selected was 0.02 inches, 0.03 inches and 0.04 inches due to their cooling times being less than a second.

2. The decision of down-selection to the SMA wire and spring was based on ease of availability. Also the specifications of the wires/springs used for the application were based on high pulling force and high deflections capabilities available, the reason being the weight of the system which it would have to withstand a later stages of design should satisfy our factor of safety along with required actuation capabilities. Our application would

require the SMA's to perform linear actuation, we performed experiments on lab scale to know its capabilities. Both the wire and springs were tested as the decision among the two would be the outcome of following experiments.

3.2 Characterization of SMA behavior

The objective of this experiment is to study the deflection of SMA springs under varying load to know about its actuation abilities as it is heated. The experiment results would form the basis of the initial design parameters to be considered for designing the mechanism.

3.2.1 SMA Springs

Experimental Setup (SMA temperature control using electric current) –

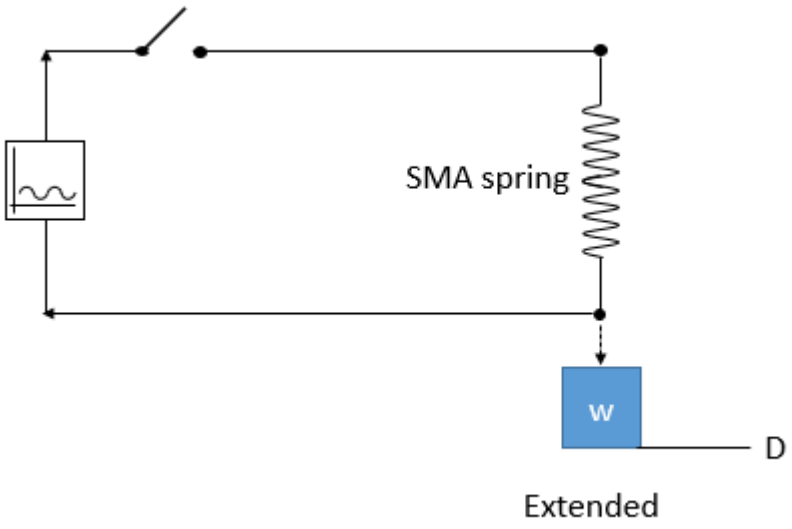

Figure 28 - SMA spring actuation schematic diagram (deactivated)

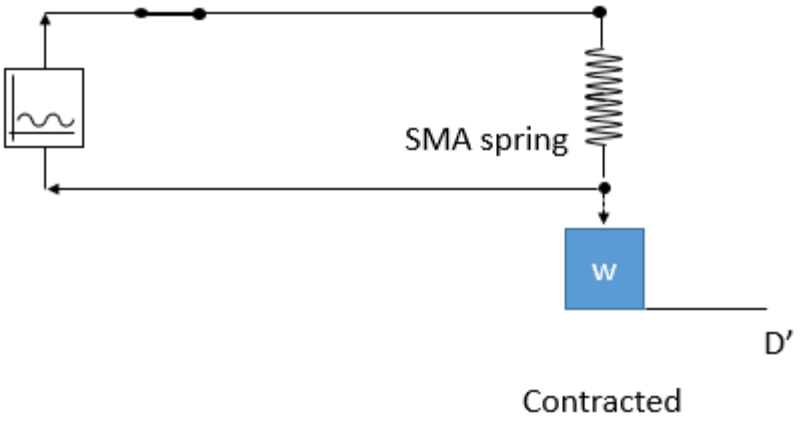

Figure 29 - SMA spring actuation schematic diagram (activated)

Deflection for the springs = D-D'

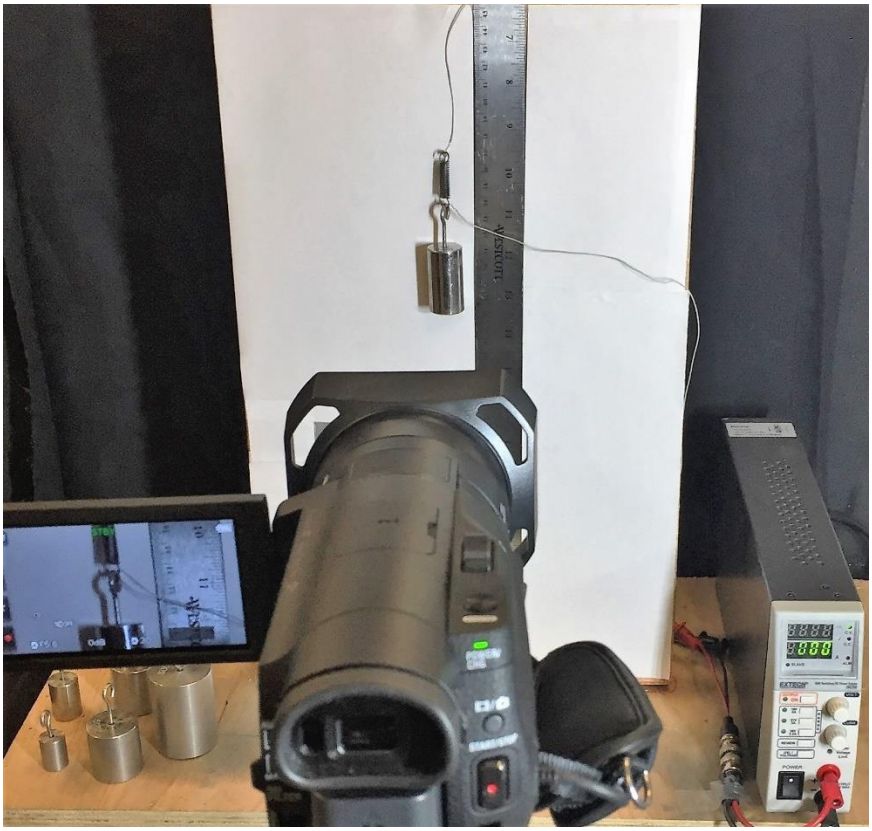

Figure 30- Experimental setup for SMA spring characterization

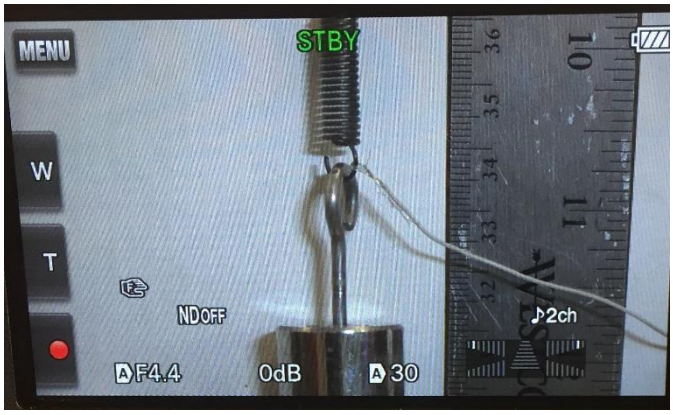

Figure 31 - Camera setup for deflection measurement for SMA spring

On a vertical wooden block, a measuring scale was mounted and fixed. SMA spring was fixed to upper end of the vertical block. The end of the springs is attached with electric wires to provide heat through a variable power source. As per the manufacturer's specification, 3 amps current for1 sec has to be supplied for complete actuation.

Procedure -

1. Current is passed through the spring initially to do away with uneven extensions.
2. Once the spring is at room temperature, reading and after load is added to the spring reading is noted.
3. Then the current is sent through the spring until it can no further contract and reading is noted.
4. The difference between the readings gives the deflection.
5. Once the spring is at room temperature, it is ready for the next cycle.

The readings from the upper edge of the weights are noted against the measuring scale.

3.2.2 SMA Wire

Experimental setup (controlled heat using current) –

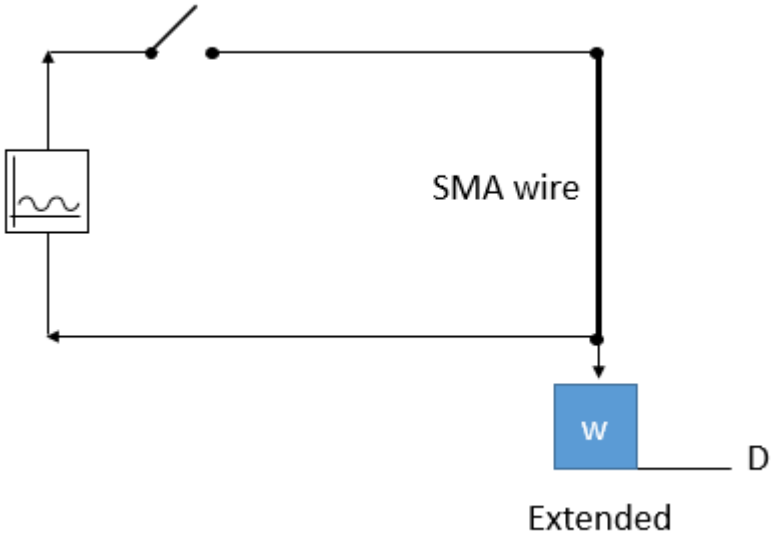

Figure 32 -SMA wire actuation schematic diagram (deactivated)

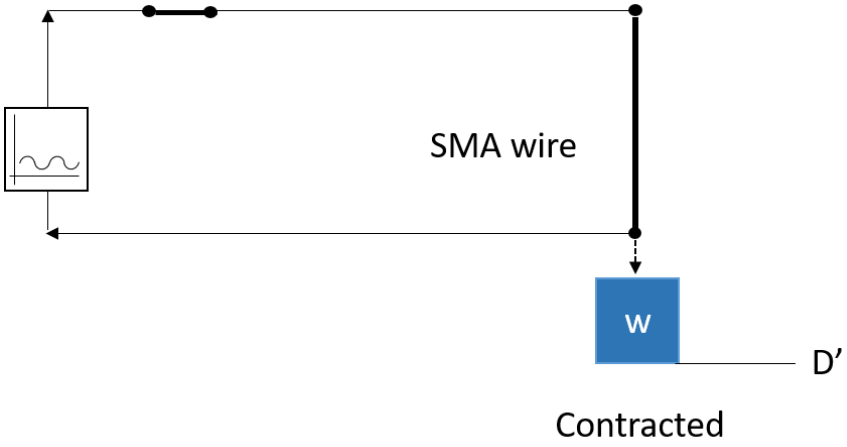

Figure 33- SMA wire actuation schematic diagram (activated)

Deflection for the wire = D-D'

Figure 34 - Experimental setup for SMA wire characterization

Figure 35 - Camera setup for deflection measurement for SMA wire

On a vertical wooden block, a measuring scale was mounted and fixed. SMA wire was fixed to upper end of the vertical block. The ends of the wire are attached with electric wires to provide heat through a variable power source. As per the manufacturer's specification, 2.250 amps current for 1 sec has to be supplied for complete actuation.

The procedure for wire actuation is identical to that of the spring. The readings for the upper edge of the crimp were noted against the measuring tape.

3.2.3 Sources of error

a. Parallax error

The parallax error in the experiments performed is due to manual loading of the weights on the center of the ring crimp. For error free readings the center of the ring crimp must be in line with the center of the hook on the weights. Therefore, the possibility of the error which might occur due to placement of the weights cannot be ruled out. In order to mitigate this error, the weights were removed after every reading in order to prevent a stack up of errors. A large sample size of readings was taken to reduce the error repeatability.

b. Environmental conditions

The environmental conditions play a significant role in SMA behavior. It has a direct effect on the cooling time of the wire/spring which in turn determines the cycle time for the whole operation. The operating temperature of the wires/springs used in the above experiment have been specified by the manufacturer at 20°C. In the course of our experiments, we observed the temperature to vary between 20°C and 22°C. To mitigate this error, multiple sets of readings were taken.

3.3 Mechanism Selection

As discussed, SMA's as wires can handle large stresses but give very small deflections. On the other hand, SMA springs can be used for larger deflection but provide a low force pulling capacity. For this reason, wires were chosen over springs. For the same deflection as of springs the length of the SMA wires have to be longer as the wires can contract millions of times for just 3-4% extension. Based on this fact we looked at different ways SMA wires can be used to give higher stroke.

Far more important to stroke is how the wire is physically attached and made to operate. Dynamics in applied stress and leverage also vary how much the actuator wires move. While normal bias springs that increase their force as the Flexinol actuators contract have only 3-4% stroke, reverse bias forces which decrease as the actuator wires contract can readily allow the wire to flex up to 7%. Mechanics of the device in which it is used can convert this small stroke into movements over 100% of the wires' length and at the same time provide a reverse bias force. The stress or force exerted by Flexinol actuator wires is sufficient to be leveraged into significant movement and still be quite strong. Some basic structures, their percent of movement, and the approximate available force they offer in different wire sizes are as follows [20].

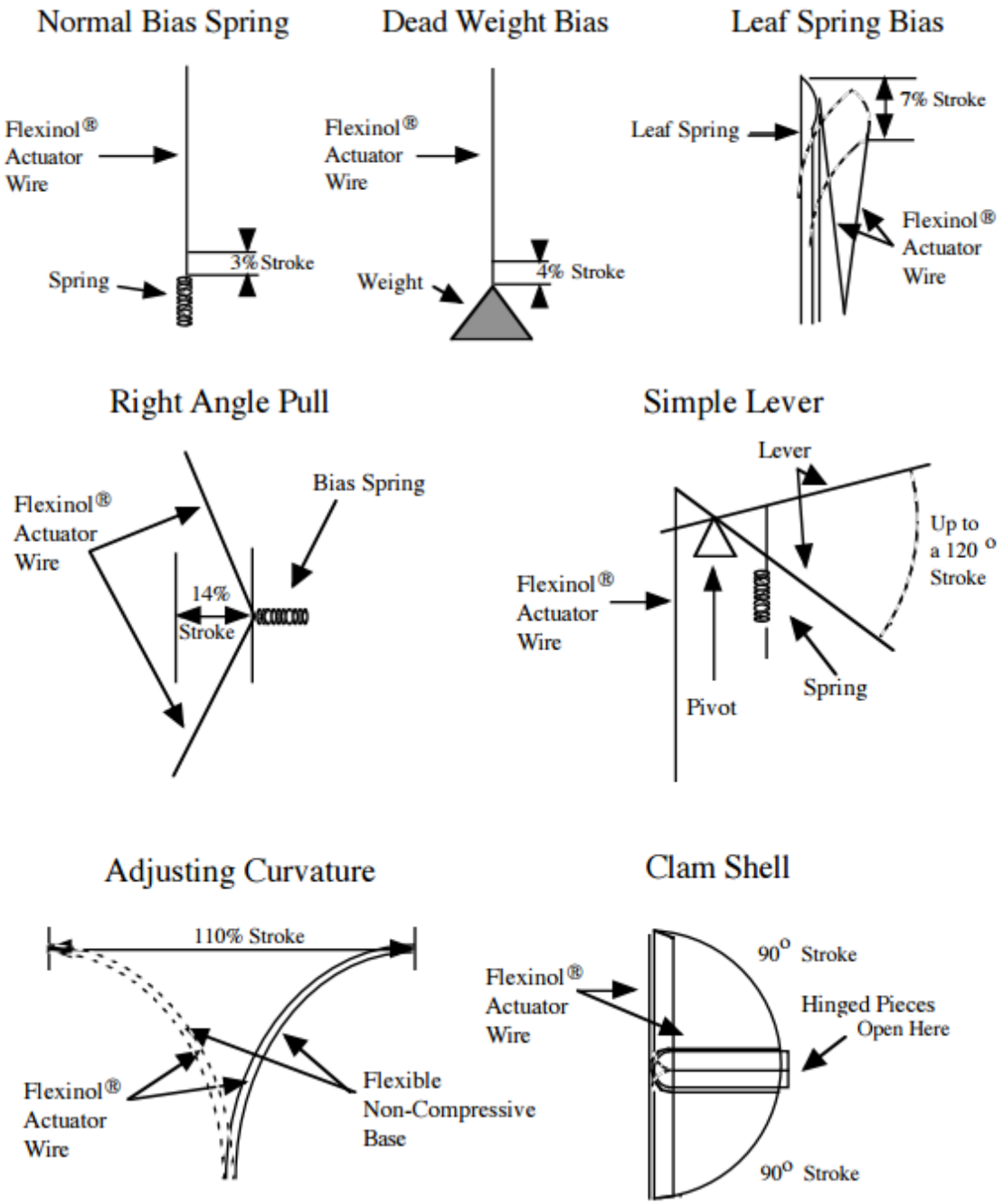

Figure 36 - Different mechanisms to obtain variable percentage of stroke [20]

	Approx. Stroke	0.003" Wire (0.076 mm)	0.006"Wire (0.15 mm)	0.010" Wire (0.25 mm)
Normal BiasSpring	3%	0.18 lb (80g)	0.73 lb (330g)	2.05 lb (930 g)
DeadWeight Bias	4%	0.18 lb (80g)	0.73 lb (330g)	2.05 lb (930 g)
Leaf Weight Bias	7%	0.18 lb (80g)	0.73 lb (330g)	2.05 lb (930 g)
Right Angle Pull	14%	0.04 lb (20g)	0.18 lb (83g)	0.51 lb (232 g)
Simple Lever(6:1ex)	30%	0.024 lb (11g)	0.10 lb (47g)	0.29 lb (133 g)
Adjusting Curvature	110%	0.06 lb (3g)	0.026 lb (12g)	0.075lb (34 g)
Clam Shell	100%	0.007 lb (3.2g)	0.028 lb (13g)	0.082 lb (37 g)

Table 1 - Force and stroke availability for different mechanisms [20]

As it can be observed, keeping the feasibility of manufacturing and also the available stroke with minimal deflection the simple lever system was chosen. It gives a mechanical advantage to have a higher resultant deflection with minimal deflection obtained from Shape Memory Alloy wire. Also provides flexibility to choose the ratio at which the lever distribution can be done and make full use of the SMA wire maximum force application.

For latching applications, the right angle pull type configuration was chosen, considering the existing applications.

3.4 Setting up design parameters

The main goal for this actuation is to implement shape memory alloy as the driving mechanism for a linear actuator for periodic motion to control the antenna. The design would take advantage of straight shape memory alloy wires to produce a deflection to keep the strain levels on the wire within 3-4 % [28].

The factors affecting SMAs are -

- Size of the SMA

The diameter of the SMA is very crucial factor to be analyzed, it affects the following parameters –

1. Resistance per unit length
2. The bias force when cool
3. The pulling force when heated
4. The maximum breaking force
5. The cooling rate (small wires cool faster than the large ones)
6. Minimum bending radius

The wire we chose for our application was the one with higher diameter as it gives us advantage on many of the above factors. Also we are using ring crimped SMA wires since bending them to crimp them tends to over strain the SMA which reduces it efficiency to work for millions of cycles. Using ring crimps helps avoiding this overstress and also the loss of wire length which would otherwise would have lost during bending and crimping. The maximum size commercially available is the 0.015 inch Flexinol wire from Dynalloy Inc. having a maximum pulling force of 2000 grams as per tech sheet from Dynalloy Inc.,

The technical information available from Dynalloy Inc. for SMA wires -

Diameter size inches (mm)	Resistance ohms/inch (ohms/meter)	Heating pull force pounds (grams)	Cooling deformation force pounds (grams)
0.001(0.025)	36.2(1425)	0.02(8.9)	0.008(3.6)
0.0015(0.038)	22.6(890)	0.04(20)	0.016(8)
0.002(0.050)	12.7(500)	0.08(36)	0.032(14)
0.003(0.076)	5.9(232)	0.18(80)	0.07(32)
0.004(0.10)	3.2(126)	0.31(143)	0.12(57)
0.005(0.13)	1.9(75)	0.49(223)	0.2(89)
0.006(0.15)	1.4(55)	0.71(321)	0.28(128)
0.08(0.20)	0.74(29)	1.26(570)	0.5(228)
0.01(0.25)	0.47(18.5)	1.96(891)	0.78(356)
0.012(0.31)	0.31(12.2)	2.83(1280)	1.13(512)
0.015(0.38)	0.21(8.3)	3.14	1.77(900)
0.020(0.51)	0.11(4.3)	7.85(3560)	3.14(1424)
Diameter size inches (mm)	Approx. current for 1 second contraction	Cooling time 158° F, 70° C LT Wire (seconds)	Cooling time 194° F, 90° C HT Wire (seconds)
0.001(0.025)	45	0.18	0.15
0.0015(0.038)	55	0.24	0.2
0.002(0.050)	85	0.4	0.3
0.003(0.076)	150	0.8	0.7
0.004(0.10)	200	1.1	0.9
0.005(0.13)	320	1.6	1.4
0.006(0.15)	410	2	1.7
0.08(0.20)	660	3.2	2.7
0.01(0.25)	1050	5.4	4.5
0.012(0.31)	1500	8.1	6.8
0.015(0.38)	2250	10.5	8.8
0.020(0.51)	4000	16.8	14

Table 2 - Technical Specifications of Flexinol Wires for different sizes [20]

- Temperature

Temperature is one of the most significant factors upon which the SMA behavior is dependent. There are two major ways to heat up the SMA's -

a. With direct heat

b. With current

We can use one of the two mentioned ways of heating. Direct heat being uncontrollable, it's difficult to have exact control over temperature. Whereas current can be controlled and thus as per the specification sheet from Dynalloy Inc. the specific current levels can be implemented to activate the wire. i.e. reach the As to Af temperatures. The current after sometime needs to be reduced as the temperature of the wire keeps increasing and it might overheat the wire causing it to lose its properties in few cycles. The cooling cycle due to Hysteresis starts at a lower temperature that the activation temperature i.e. from Ms to Mf. The SMA wire chosen has an activation temperature of 90 degrees for which the current requirements are 2.250 Amps and 5.5 V voltage. According to the tech sheet, it will increase the temperature of the wire to 90 degrees celsius in a second and thus contraction will happen within that second.

- Initial Shape setting

The shapes we considered were the SMA in the form on straight wire and also the spring. The wires give higher pulling force at the cost of stroke while the springs give significant stroke at the cost of pulling force. Essentially a wire is more efficient than a coil form since there is no loss of force due to transverse and torsional shear. Other factors also include higher current requirements by the SMA springs and higher time to cool when compared

to the SMA wires. Therefore, the SMA wire was selected over the spring for this application.

- Stroke

The purpose of the linear actuator is to have a good amount of available pulling force along with a reasonable stroke length which would cater to achieving a fixed angle as per the aim of the project with a sense of controllability. Small strokes make it difficult to control since small increments in current give rise to bigger deflection. Another factor that dominates this parameter is the hysteresis associated with the shape memory element. Also due to hysteresis the actuation temperatures form As to Af are different from Ms to Mf, the range over which the actuator can be controlled is higher than systems following linear paths.

- Environmental conditions/ cooling conditions

Once heated, to get the relaxed martensite phase of the wire it must be cooled. The rate at which it is cooled determines the overall cycle rate. Therefore, the material in contact with the wire acts as a heat sink. Air, liquids, coatings and other materials including crimps has significant heat extracting effects. Still air acts as the basic heat sink, whereas running air, immersing it in water/glycerin mixture will increase the cooling effect greatly.

For space application due to presence of vacuum which acts as a poor heat sink since there is nothing to take away the heat, the SMA wire if in contact with a conductive mass will increase the cooling rate.

- Stress/Strain

The low achievable strain levels from SMA make them ideal for microscopic application rather than macroscopic applications. Though the stress the SMA wires can withstand for a given size is quite high, it still lacks the high load pulling capacity for macro applications.

The strain levels which can be achieved using SMA elements are pretty low i.e. for 8% strain levels it can work a few cycles, for 5-8% it will work for around thousand cycles and for 3-4% strain cycles it will for hundreds of thousand cycles.

- Bias force

The bias force can be defined as the force required to deform or extend a cooled SMA wire to bring it back to detwinned martensite state. A subsequent heating of the material to a temperature above Af will result in reverse phase transformation (martensite to austenite) and will lead to complete shape recovery, as shown in Figure (5). The above described process results in manifestation of the *Shape Memory Effect* (SME). Bias force is also regarded as a way to maintain tension in the SMA wire after cooling and maintain a constant extension so that it helps giving a significant stroke.

The various ways in which bias force can be applied are as follows –

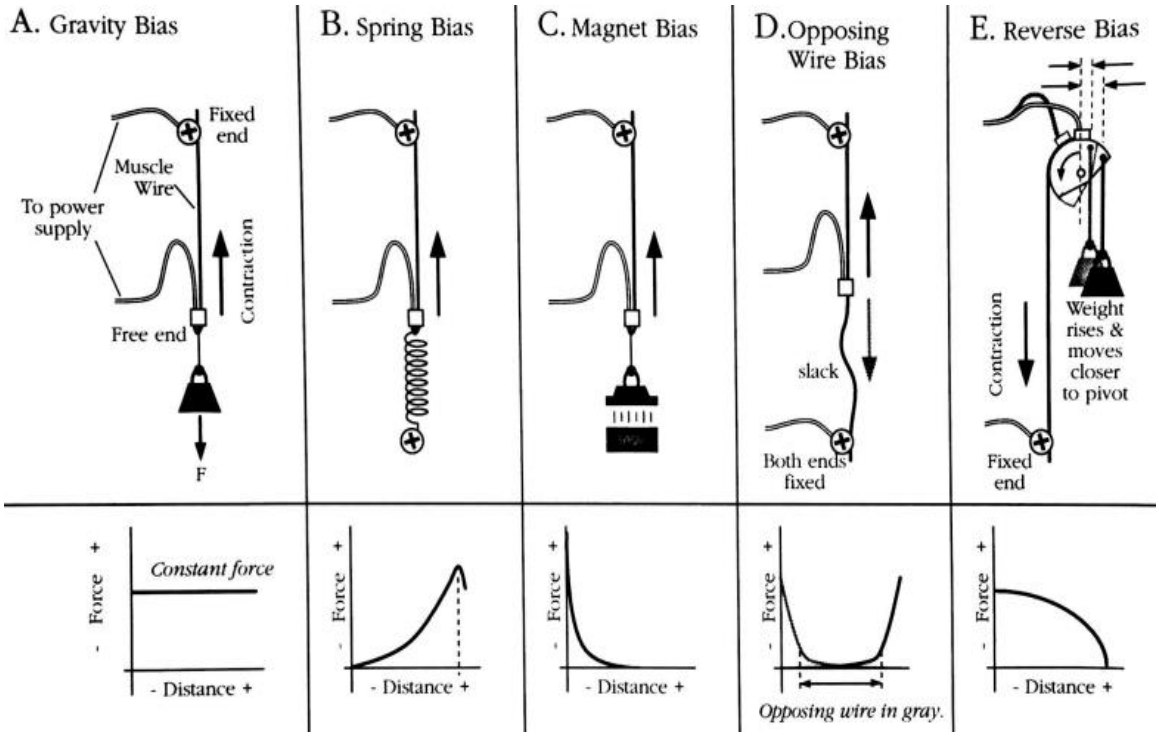

Figure 37 - Different ways to provide bias force [28]

- Cycle rate

Cycle time is defined as the amount of time needed to actuate and relax a shape memory element and the cycle rate as the amount of cycles the actuator can perform per unit of time. The cycle time can be divided into two: heating or actuation time and relaxation or cooling time. Since the cooling time for SMA wires is less when compared to springs the cycle time for them is low. Also actuation is done electrically as per the specifications the wire will be chosen with regards to the maximum pulling force and cooling time. Cooling time depends significantly on the external temperatures. We will also be choosing HT wire, since the cooling time for the HT (High Temperature) wires is lower than LT (low temperature) wire. The cooling time for the wire used for our application is 8.8 secs. Also the cooling time for the wire used for latching mechanism is 0.9 secs.

Cycle time calculations -

1. Heating the 20 cm SMA wire - 1 secs
2. Heating the SMA wire used for latching - 1 sec
3. Cooling of SMA wire used for latching - 0.9 sec

Total Cycle Time - 2.9 sec

The cooling time for 20 cm SMA wire has not been added since, after full actuation we don't require it to operate until the next operation is within 8.8 secs.

3.5 Strengths of Multiple Muscle Wires Lifting in Parallel

Wire size (μm)	Quantity	Total lift (kg)	Total power (Watt)
50	10	0.35	1
50	50	1.75	6
50	100	3.5	13
50	250	8.75	32
100	10	1.5	5
100	50	7.5	24
100	100	15	49
100	250	37.5	122
150	10	3.3	8
150	50	16.5	40
150	100	33	80
150	250	82.5	200
250	10	9.3	20
250	50	46.5	100
250	100	93	200
250	250	232.5	500

Table 3 - Tradeoff Between Multiple Wire Use for Force Vs Power

Using bundle of wires gives the advantage of achieving same lift force for any application with relative low power. For ex. From the table above using 50 wires of 250 μm diameter give total life force of 46.5 kg with 100 watts power, whereas 250 wires of 100 μm diameter provide a lift force of only 37.5 kg with more power i.e. 122 watts. Thus, setting tradeoff choosing appropriate size vs quantity can help us achieve optimum lift for minimum power.

3.6 Prototype Design

This section discusses the working of the prototype design through CAD model view and provides with insight on the calculations for the selected dimensions.

3.6.1 Experimental Setup for linear actuation

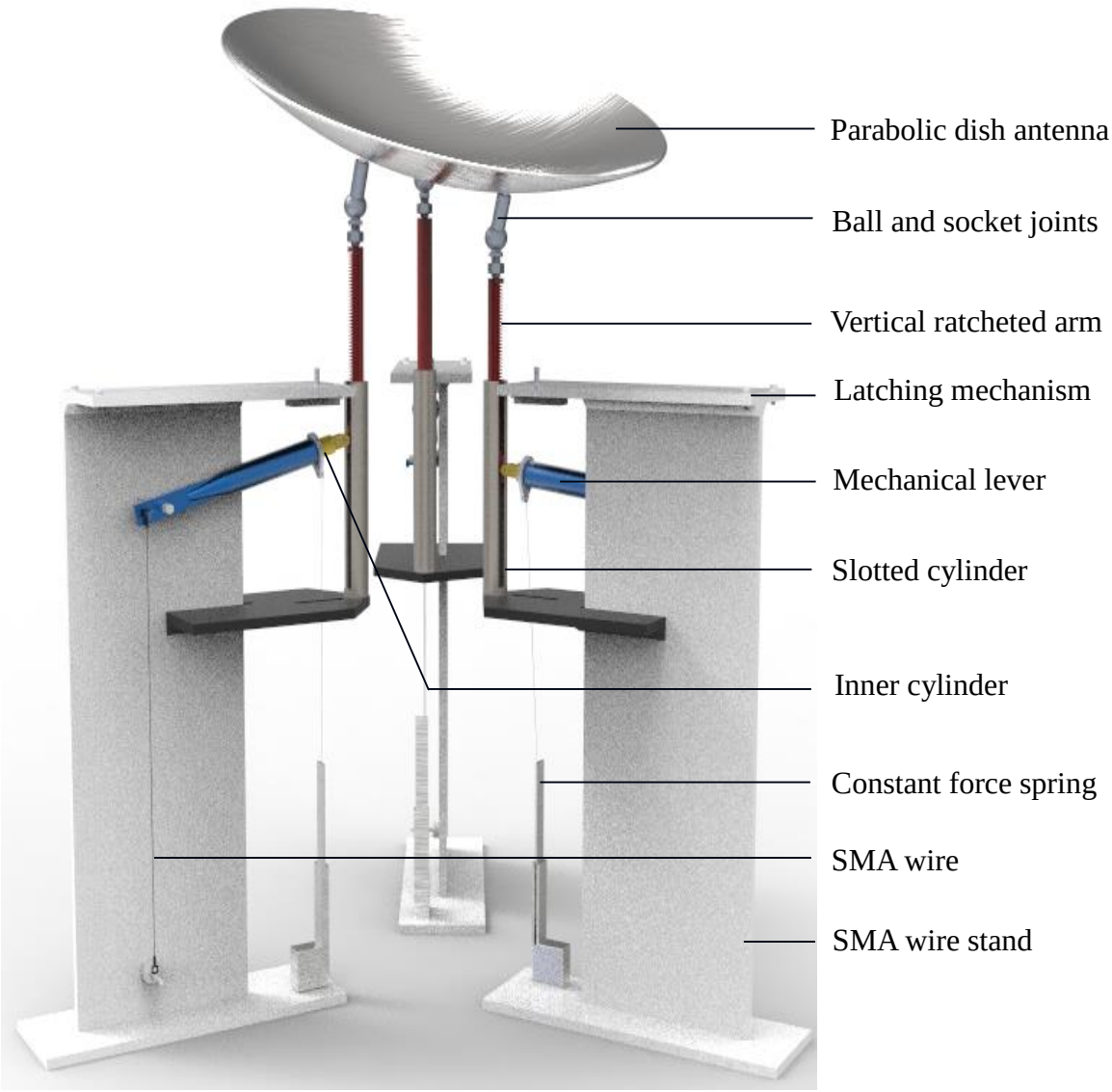

Figure 38 - Full Assembly view of the mechanism

The above picture shows the CAD model view of the whole assembly of the antenna pointing mechanism based on SMA straight wires as sources of linear actuation.

A mechanical lever type structure was chosen to amplify small SMA deflection into a larger value. This larger value is defined by the mechanical advantage offered by the configuration. The construction of the mechanism is as shown in figure (38).

Figure 39 - CAD model view of mechanical lever and linkages

The shorter end of the lever is attached to one end of the SMA wire while the other end is fixed to the body of the system on the bottom. The SMA's have a tendency to contract on heating which tends to pull the lever downwards and rotate about the fulcrum.

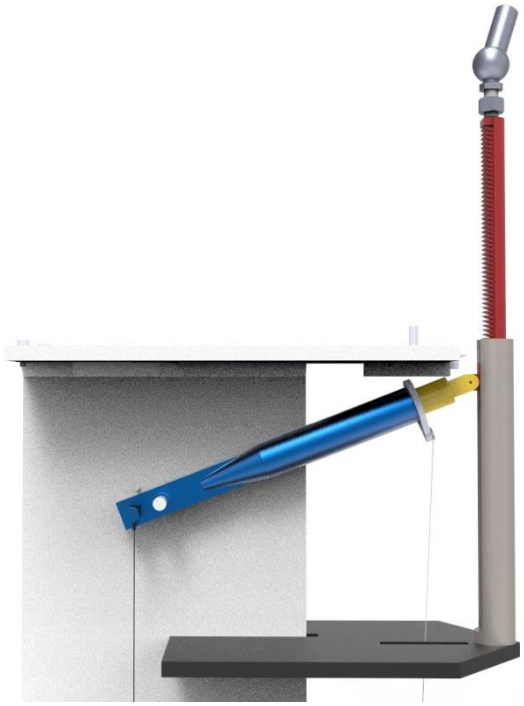

Figure 40 - CAD model view showing Vertical ratcheted arm and other linkages

As can be seen in the figure above, to convert this circular motion into linear motion, the longer end of the lever has a construction of a telescopic cylinder as a part of its body length. The inner cylinder of the telescopic body has a pin joint with a cylindrical slot having the ability to oscillate inside a slotted cylinder. This slot is attached to a vertical ratcheted cylindrical column which on the other end is attached to the antenna as shown in figure (40).

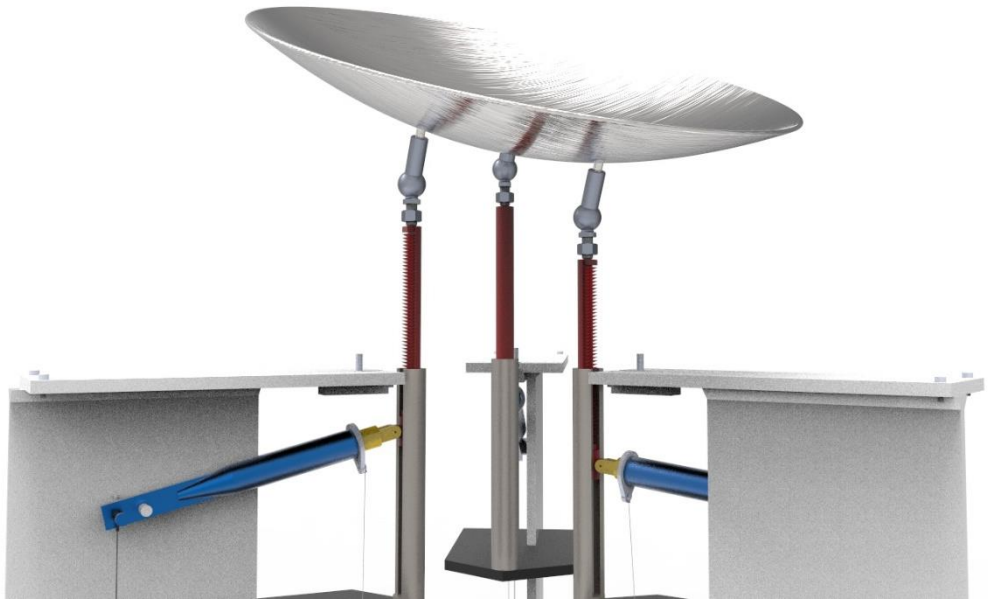

Figure 41 - CAD model view of three vertical arms responsible for angular movement of antenna

In order to control the antenna's movement, its facing plane is modulated by adjusting three control points. The elevation of these points is controlled using SMA actuated movement and thus the angular movement of the antenna by a certain angle.

For the mechanical lever construction from the figure (42, 43) the division of lever in a certain ratio is determined by the size/diameter of the antenna and the amount of angular movement to be achieved. The target angle of tilt was set at 45 degrees according to which the ratio required would be 1:10.

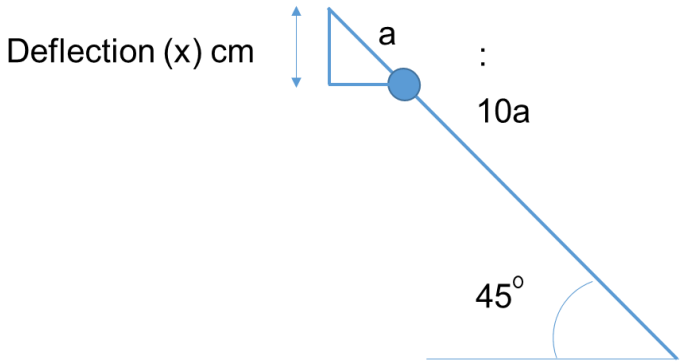

Figure 42 - Schematic for Geometric construction of mechanical lever

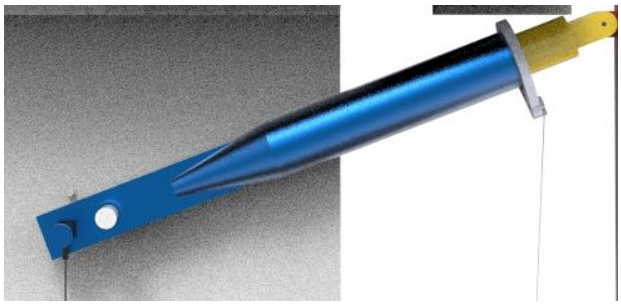

Figure 43 - CAD view for geometrical construction of mechanical lever

The above figure shows a simplified schematic of the mechanism. The following calculations were carried out:

Assuming the short and long lever arms to be of lengths ‘a’ and ‘10a’ respectively,

$$deflection\ (x) = (a \times \sin 45°)cm = (0.7071a)cm$$

By observing the Characterization graph on figure (51) for the SMA wire, it can be concluded that at 900 grams bias force, we get 0.7 cm deflection which lies in the range of 3-4 % of wire of length 20 cm. This is the reason we chose 20 cm wire. Further, by similarity of triangles the deflection is magnified by 10 times due to lever ratio.

Now, for 45° the defection required was 0.7071cm, but since the maximum consistent deflection noted from the SMA experiments is 0.7 cm the new max angle which can obtained can be calculated as follows -

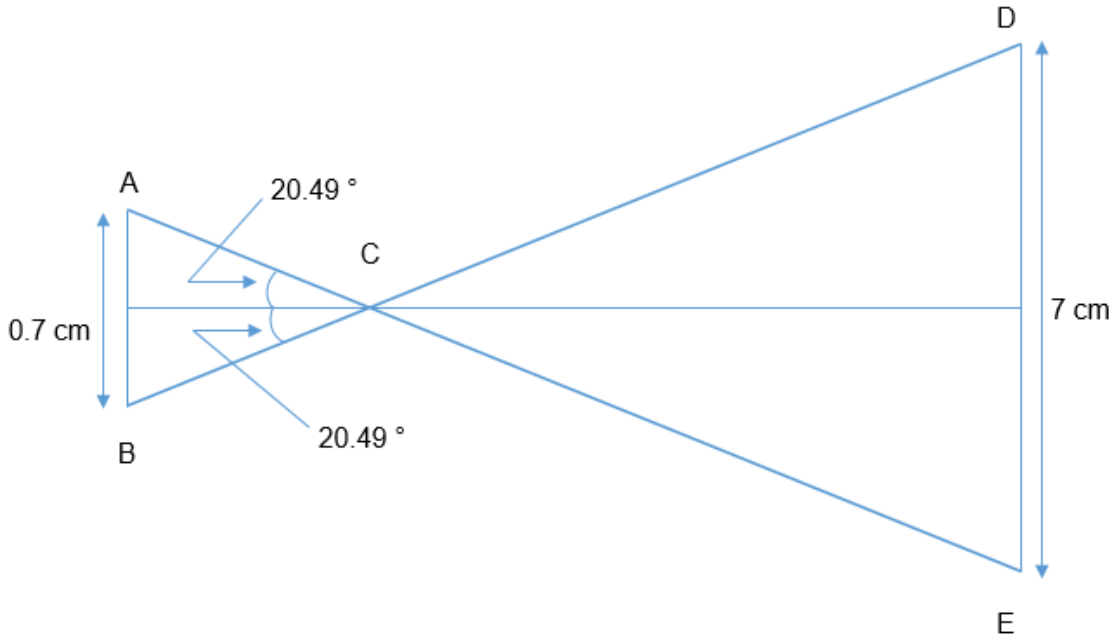

Figure 44 - Schematic showing linear displacement of vertical arm and angle achieved

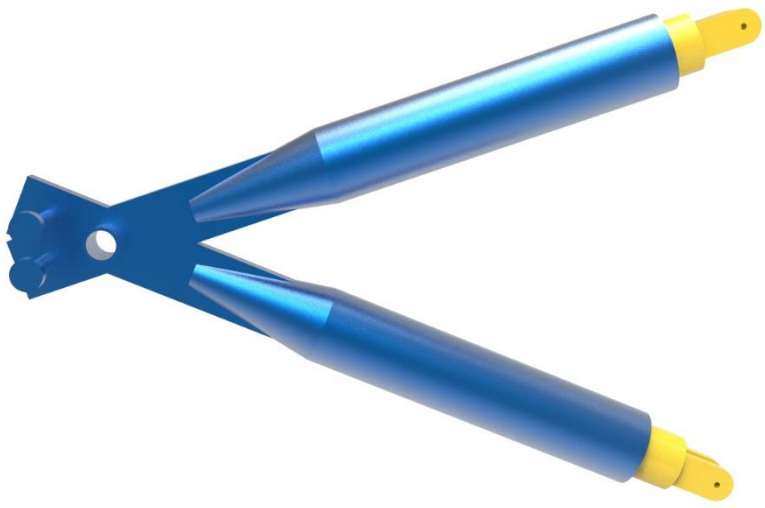

Figure 45- CAD view for linear displacement of vertical arm and angle achieved

Therefore, the total angle of deflection for the actuators is 40.98˚. To attain 45˚angular tilt for the antenna, the vertical actuators have to be adjusted and placed on the periphery of the antenna according to following calculations –

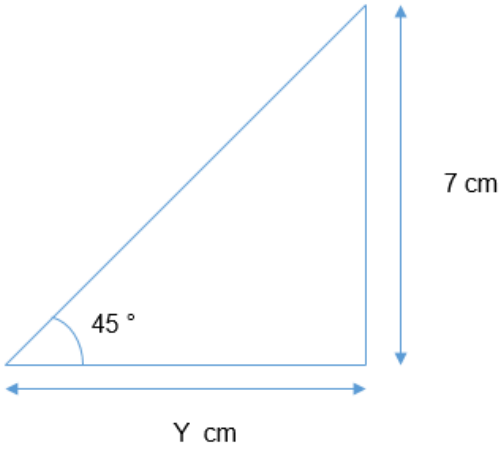

Figure 46 - Schematic for movement of antenna movement by vertical ratcheted arms

The value of Y is 7 cm. This distance is the distance between the virtual circles on the periphery of which these actuator assemblies will be placed. To determine the distance between each actuator, we follow this procedure –

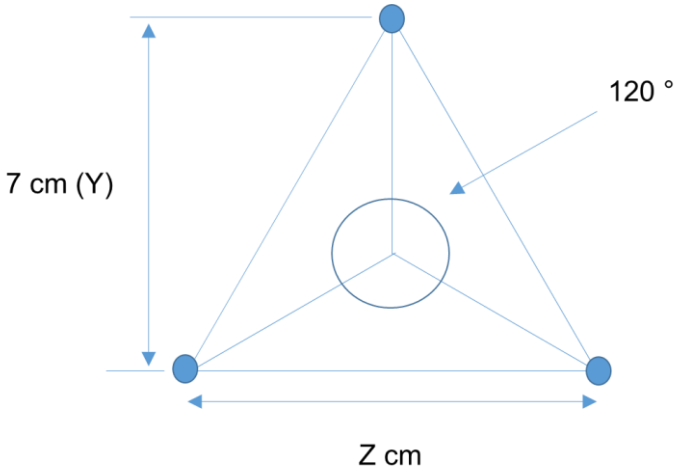

Figure 47 - Schematic for Spatial arrangement of vertical arms of the Antenna surface as seen from top

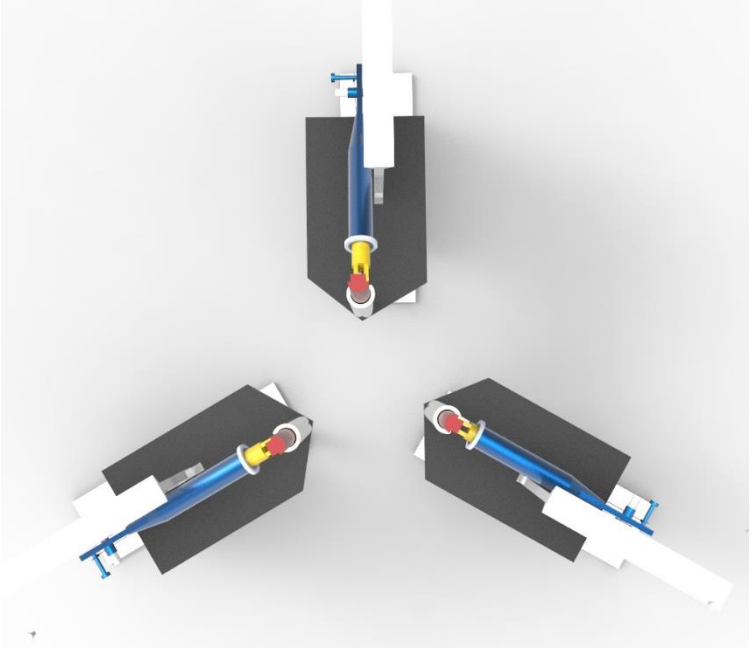

Figure 48 - Spatial arrangements of the 3 vertical arms

By trigonometry laws, the value of Z equals 8.08314 cm. Therefore, the system defined will have the ability to move ±45° elevation with 360° azimuth angle by the simultaneous control of the 3 vertical actuators.

3.6.2 Experimental Setup for latching mechanism

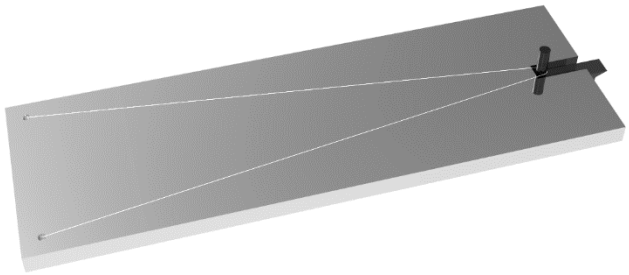

Figure 49 - Latching mechanism

The latching mechanism serves the purpose of locking the antenna to the desired position by retracting a latch pin. The vertical ratcheted arm has ratchets on its body based on the geometry observed from figure (49). The 7 cm vertical distance is divided by 45 degrees to have ratchets at a distance 0.155 cm which is equivalent to one degree. Thus making the system of 1 degree step size. The SMA wire length was chosen based on the construction of the assembly for the linear actuator and right angle pull mechanism shown in figure (38).

CHAPTER 4

RESULTS AND DISCUSSIONS

This section discusses the various experiments performed on the SMA's and the experimental prototype to determine characteristics affecting its working as a product suitable to work in space. The obtained results are followed by discussions to justify the significance of obtained traits and conclusions are drawn accordingly.

4.1 SMA Characterization studies

4.1.1 For Springs

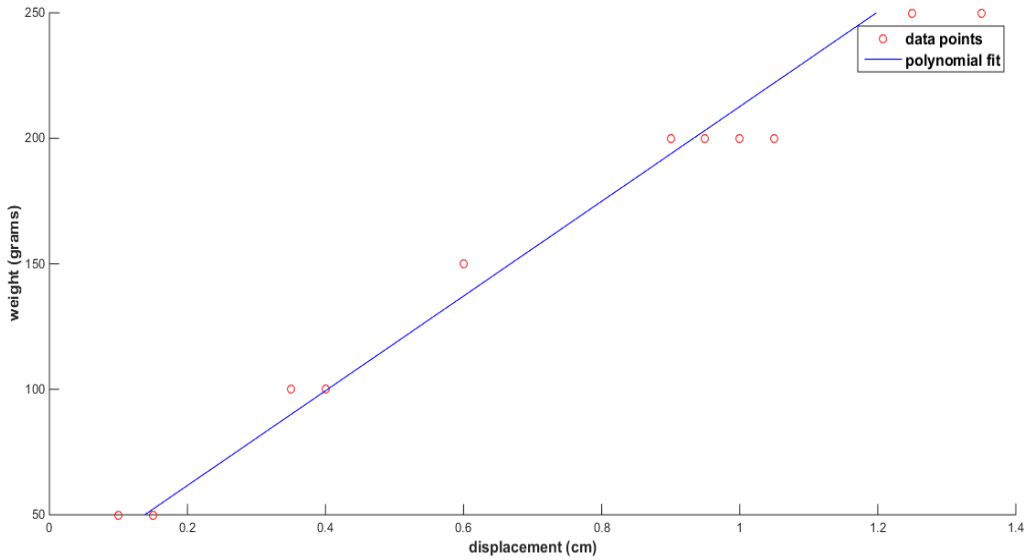

Figure 50 - Weight vs Displacement curve for SMA spring

The graph in figure (50) shows linear behavior which concludes that the SMA spring has a defined behavior at specific loads the spring is subjected to. 10 sets for each reading were taken to adhere to the precise behavior of the SMA spring for the application. Springs are characterized by stretch ratio. Stretch Ratio "SR" is defined as length "L" over the solid length "SL", in any state, hot or cold. For example, a spring with a SR of 4 cold and 2 hot, assuming a solid length "SL" of 10mm would then be 20mm hot, and 40mm cold. Spring

used for experiments was 0.020 inch Flexinol Spring from Dynalloy Inc. for which the hot and cold stretch ratio is 16 and 7. As per the characteristics of the springs, the maximum size spring has a pulling force of just 200 grams. The amount of current required for these springs is higher for the same amount of pulling force when compared to straight wires. Another reason for not using springs is its ability to provide force enough to withstand momentum changes for heavier systems. Therefore, the springs were not considered for the application.

4.1.2 For SMA wire

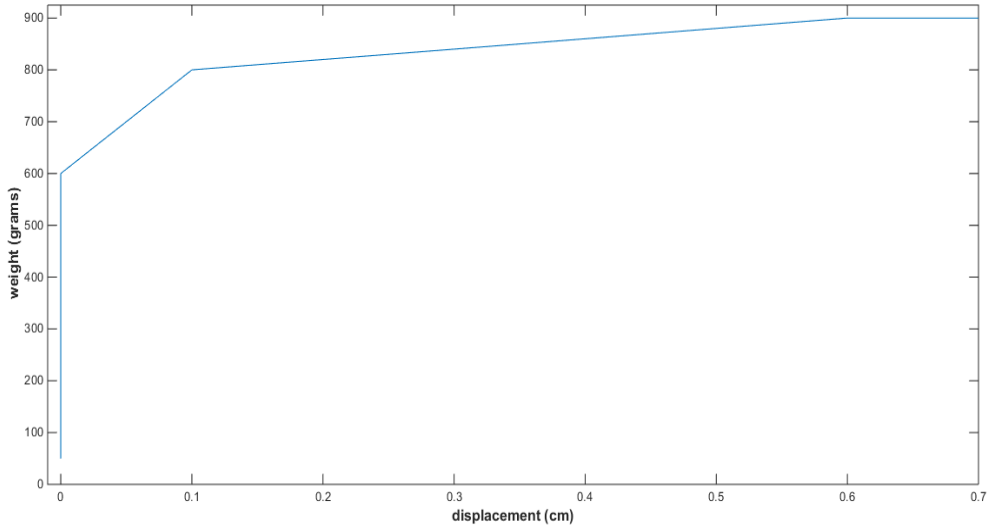

Figure 51 - Weight vs Displacement curve for SMA wire

Keeping the range of force requirements in focus, the SMA wire with highest strength is chosen for observing the general trend with varying load.

From the figure (51) the variation of the deflection follows a nonlinear path and thus with the further increase in load it is difficult to predict the deflection. This makes it uncertain for the wires to be used with accurate specifications to attain exact required

actuation stroke. Any kind of overstress or overstrain can affect the performance of the actuator. Using wires with proper heating/cooling conditions with precise bias force can cater to the needs of the system. The maximum deflection of the wire at recommended bias force i.e. 900 grams is 0.7 mm, which lies in 3-4% range (to avoid overstrain) of SMA wire of length 20 cm. The availability of the SMA wires for a wide range of pulling force and also low current requirements make their use ideal for our application.

4.1.3 Determination of wire size for latching mechanism

As the wire cools down, the constant force springs pull down the mechanical lever. The mechanical lever linked with the vertical ratcheted arms in turn starts to reconfigure the antenna in initial position (i.e. 0 degree with the normal). The speed of downward movement of the vertical arm should be less than the speed with which latching takes place for successful latching. Experiments were conducted to determine range of speed of the vertical arm during cooling phase of the SMA used for linear actuation.

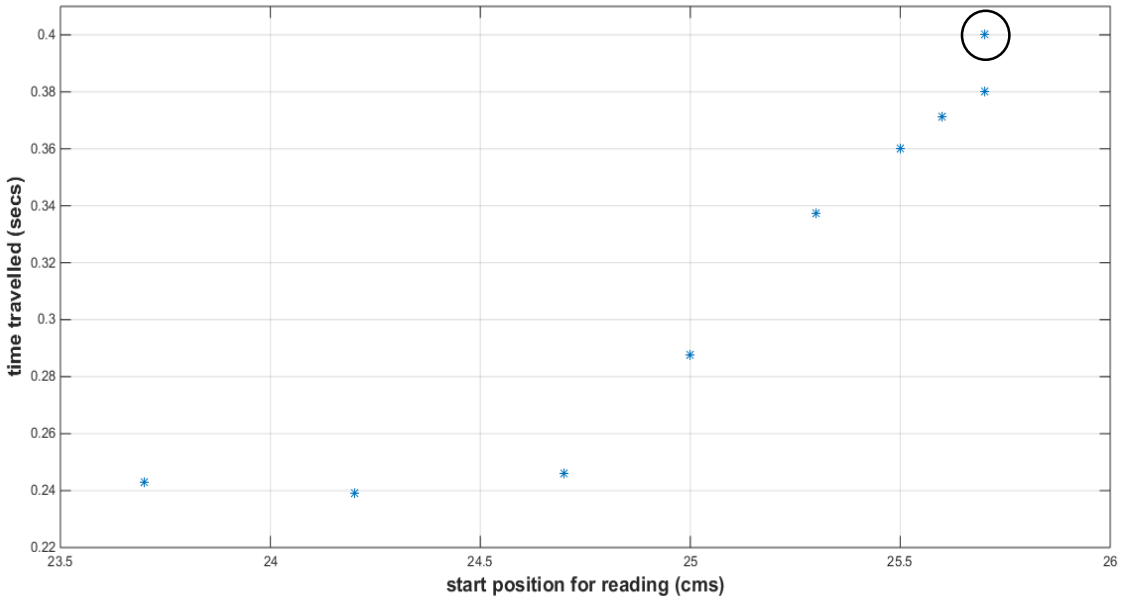

Figure 52 - Maximum speed consideration for choosing SMA wire for latching

Based on the results, calculating the time of passing 1 teeth of ratcheted actuator is given by –

Distance between each tooth – 0.155 cm

Maximum speed of the downward motion – 0.4 cm/sec

Time for passing 1 tooth (i.e. 1 degree equivalent distance) = 3.875 secs

Thus, the SMA wire with cooling time less than 0.3875 has to be chosen. SMA wire with 0.002 inches with cooling time 2 secs is selected for the application, the decision also takes into consideration the availability of bias force spring available commercially.

4.2 Demonstration of SMA based pointing and latching mechanism –

System Diagram for the experimental setup –

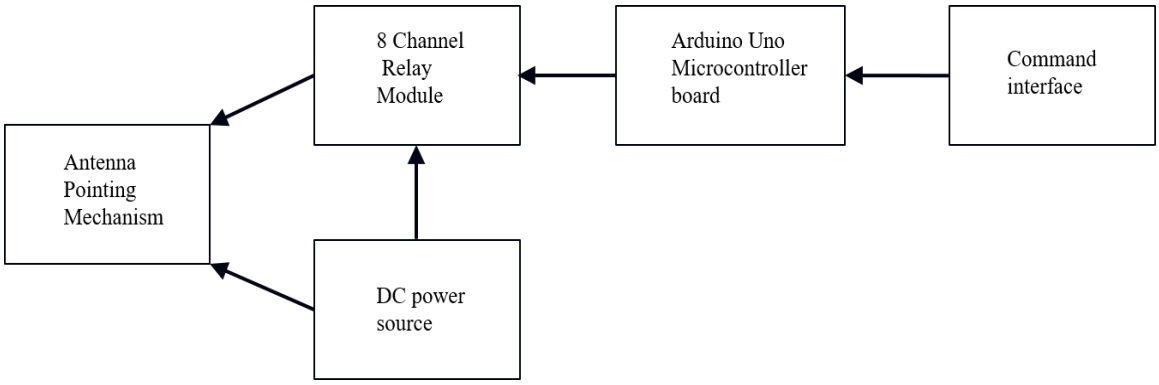

The complete system experimental setup is as shown -

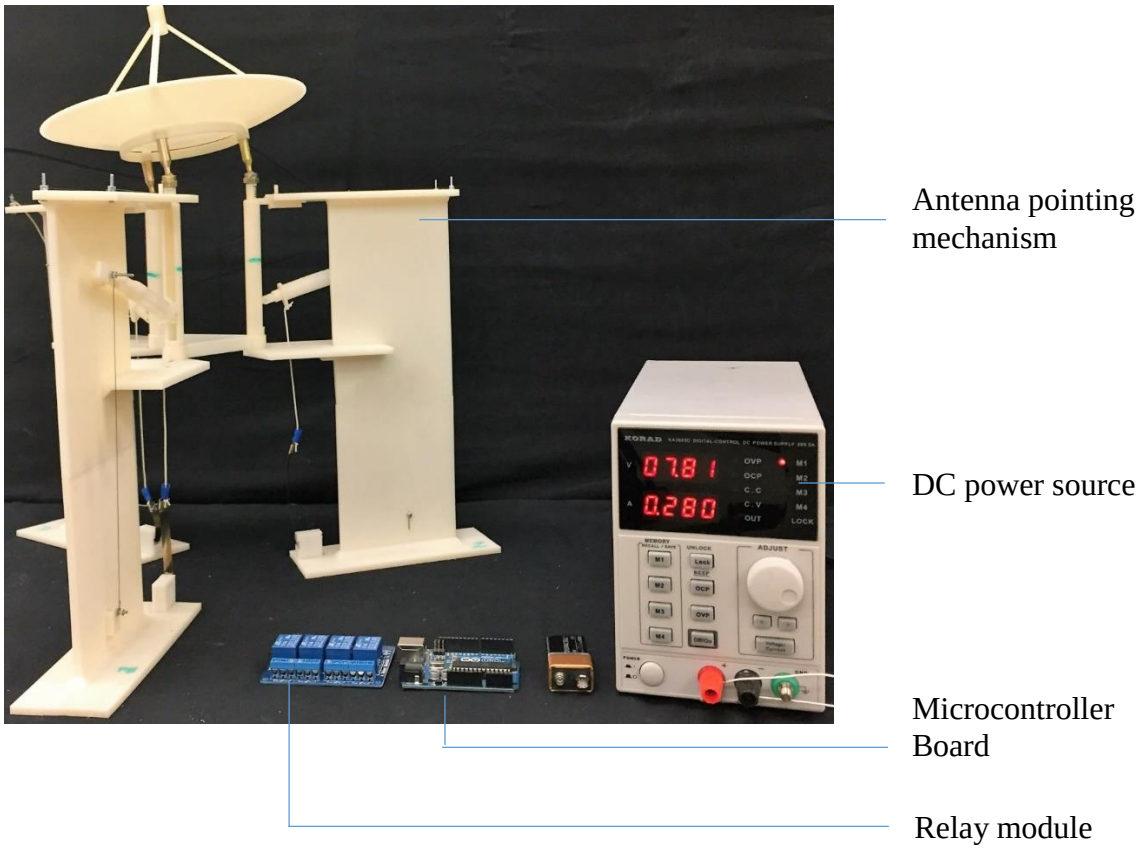

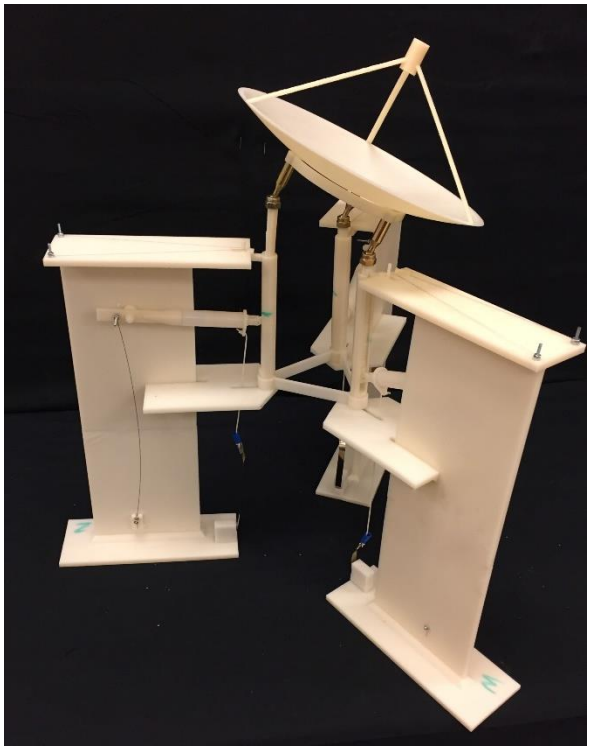

Figure 53 - The configuration for one of antennas extreme position

The following shows the working on mechanism for 1 cycle –

1. Unlatching the ratcheted actuator

On the command for a given angle to be achieved, the latched vertical actuator holding the antenna at a specific angle unlatches.

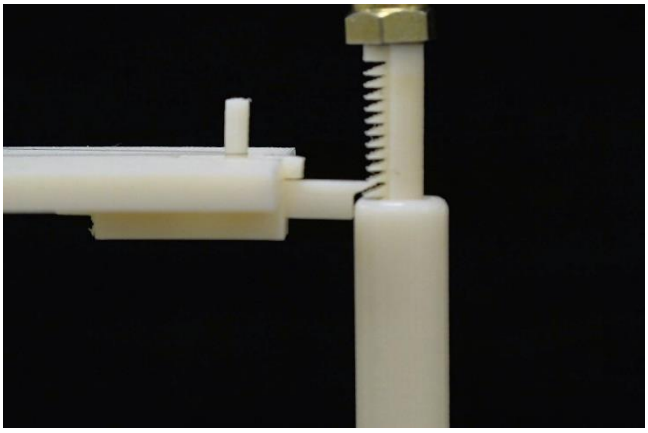

Figure 54 - Latched

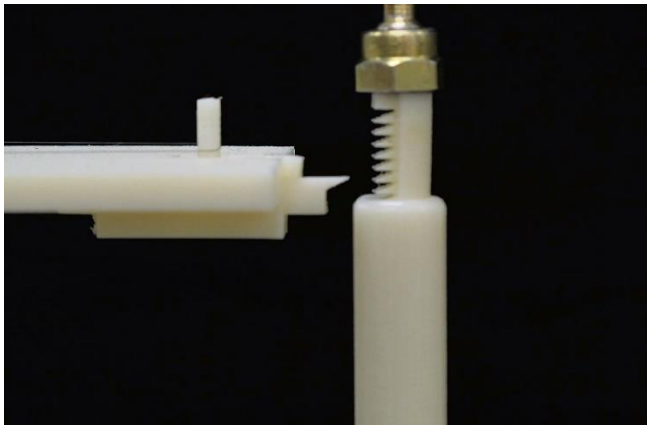

Figure 55 - Unlatched

2. The vertical ratcheted actuator is activated the moment it gets unlatched and moves up due to the contraction of the SMA wire.

Figure 56 - Initial configuration when antenna was latched

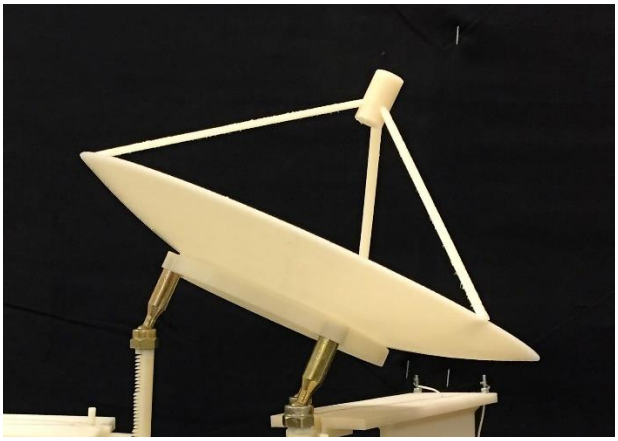

Figure 57 - Final Configuration

3. The SMA wire after being activated for 1 sec, achieves highest possible tilt angle and then begins to cool. This cause the normal angle made by the antenna to drop as the wire cools down, and bias force mechanism (constant force spring) pulls the actuator assembly towards its direction.

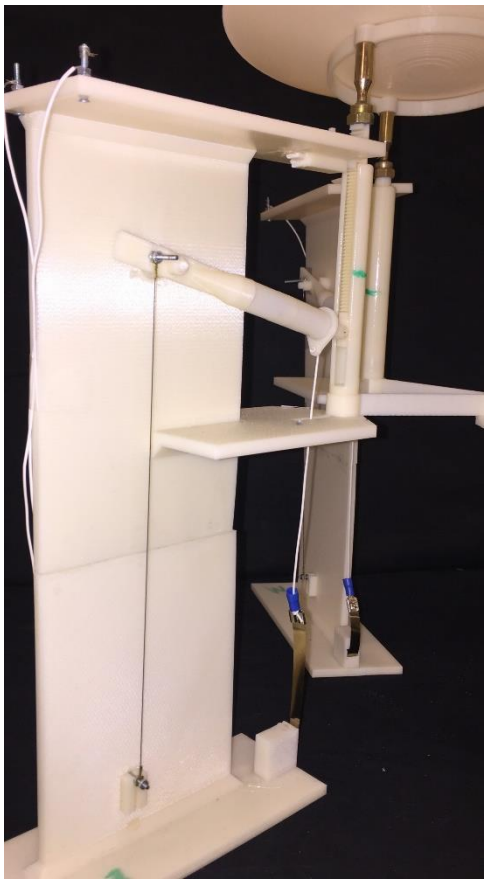

Figure 58 - Bias force springs pulling the actuator

4. As per the command, the moment vertical displacement corresponds to required pointing angle, the latching mechanism gets activated and locks the movement of vertical actuator. Thus achieving the desired pointing angle.

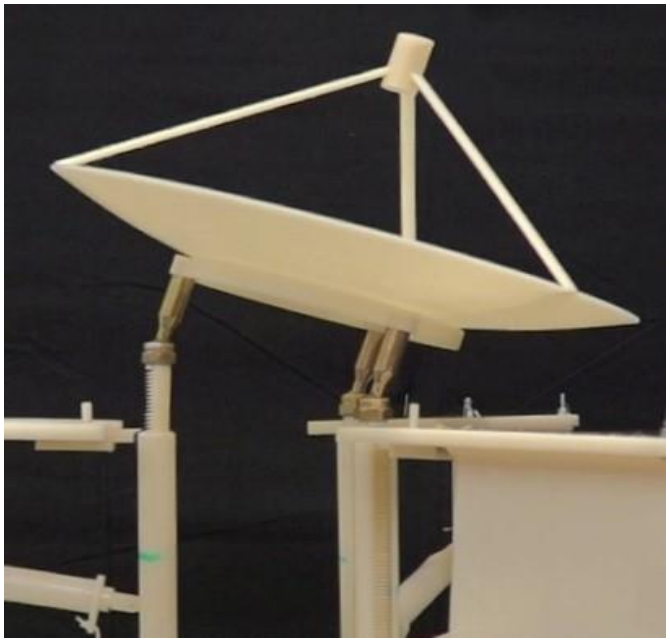

Figure 59 - Downward motion of the vertical ratcheted arm

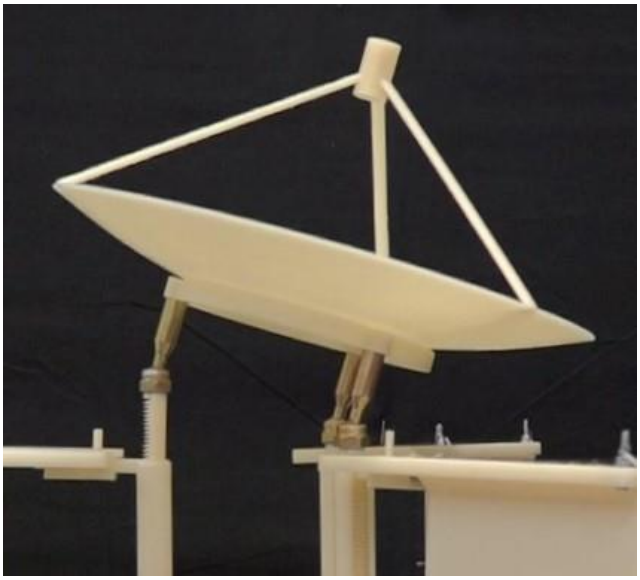

Figure 60 - Latched at desired angle

4.3 System and Subsystem Repeatability

Any pointing mechanism is required to maintain consistency to provide precise pointing over a large number of cycles. For the setup, the required angle depends on the time at which the latching takes places along with the movement of the linear actuator,

Experiments were performed to analyze the repeatability of the latching mechanism for varying latch time delays, current being provided to the wire for 1 second.

The pointing assembly consists of two major subsystems:

a. Latching mechanism

b. Linear Actuation system

Repeatability tests were performed on each of the individual subsystems and their respective contributions to the system as a whole.

4.3.1 System Level Repeatability

The graph below shows the cumulative error vs number of cycles graph

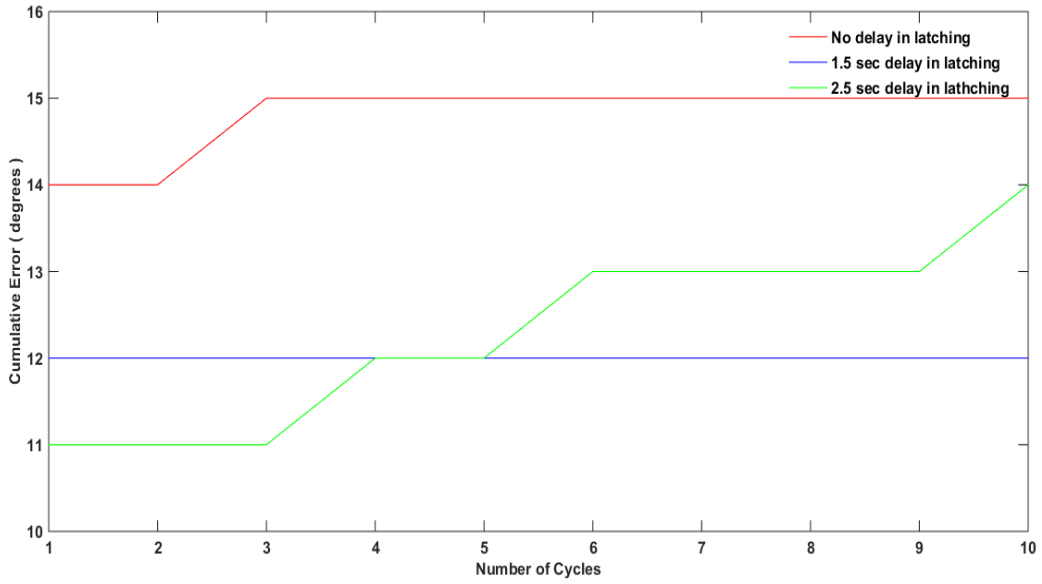

Figure 61 - Cumulative error vs Number of cycles for system

As shown by the figure (61), in the case with no delay in latching, there is a 1 degree cumulative error over 10 cycles. Similarly, in the case of a 1.5 second delay in latching no error is observed over a period of 10 cycles. In the third case, for a 2.5 second delay in

latching, the error propagates by three degrees cumulative for 10 cycles. Further the uncertainty in the error of all the three cases is due to the error sources present in the system. The different sources of error are –

1. Design and Manufacturing Errors

Prototypes for the experimental setup were manufactured using extrusion molded 3D printing which limits the surface smoothness by 0.1 mm. The frictional losses between the surfaces, provides uncertainty in its working behavior in every cycle. The movement of vertical ratchetted arm inside the slotted cylinder, and the movement of the mechanical lever with a partial cylindrical body are two major sources of error in this regard. Therefore, particularly in 3rd cases, the cumulative error compared to rest of the two cases is more due to the increase in travel time of vertical actuator, this gives more time to create more frictional losses and thus provide error in the amount of angle to be achieved.

Further, taking into consideration the 1 degree error in cases of first cases which ideally should not exist since the vertical arm is latched at its maximum travel point, in all possibility eliminating the error due to frictional losses discussed above, is attributed mainly to the latching pin design. The improvement in the design such that the latching is due to the tip of teeth touching each other can be discarded and achieving normal interlocking will mitigate this type of error.

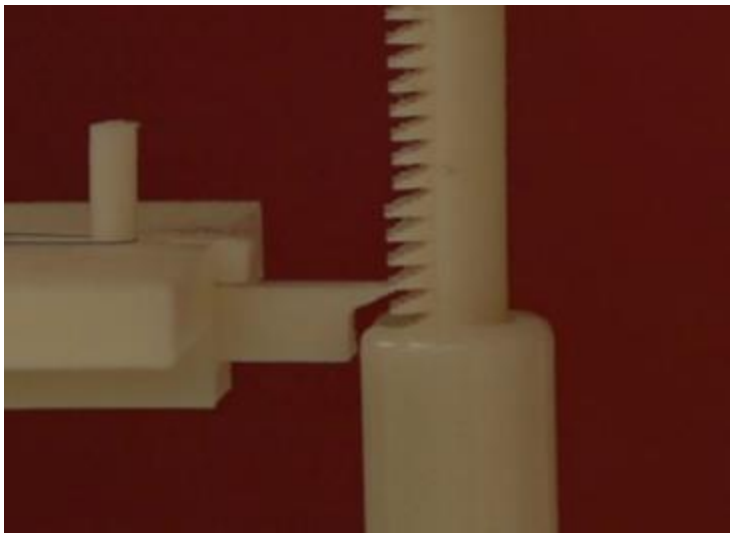

Figure 62 - Tip to Tip latching

For the system as a whole, precise manufacturing using materials like ceramic would help reduce the errors due to plastic body along with electricity and heat conductivity issues. The base of vertical cylinders, if manufactured as a single platform would mitigate levelling issues. The use of metallic wires to link the lever and constant force springs avoiding the possibility of expansion due to tensile force can further improve the accuracy of the system.

2. Heating/Cooling of SMA wire –

The tilt angle obtained depends on the contraction of the SMA wire, the activation temperature of the wire, the amount of time for which it is heated and time for which it is cooled. The amount of time for which the current is sent.i.e. 1 sec is controlled by a micro controller and helps achieve precise time gaps between successive cycles. The cycles are based uniformly on controlled cooling times as per specifications provided by the SMA manufacturer, Uniform cooling times would ideally ensure same SMA temperatures.

However, irregularities due to variable ambient temperatures and heat dissipation may lead to errors in deflection obtained.

The ways to mitigate these errors can be coating the wire with materials like Silicon (BIW P/E 5636-L-G20 WHITE SILICONE WIRE INSULATION) to improve the heat dissipation and reduced cycle time [29]

3. Positioning/working of the constant force spring –

A constant force, is a roll of pre-stressed strip which exerts a nearly constant restraining force to resist uncoiling. The force is constant because the change in the radius of curvature is constant [30]. Its initial elongation by a given amount is necessary for proper working the spring. Also the assembly used to fix the spring is significant in its working as it acts as a casing to elongate and swirl back in a restricted space. They act as potential sources of error since they are the only bias force mechanisms on the system and directly affect the contraction/elongation of the SMA wires. These springs also determine the velocity at which the vertical actuator will travel down and thus affecting the latching mechanism design. Therefore, the errors in the design of 3d printed casing, the surface smoothness it offers for springs to swirl without delay, and its position where it is being used can potentially be sources of error. The way to mitigate these errors can be using constant force assembly manufactured directly from vendors, and positioning the assembly such that the movement of the spring ribbon is parallel to its body and not twisted due to uneven forces.

4.3.2 Subsystem level errors

Repeatability studies at subsystem level:

1. Latching Mechanism:

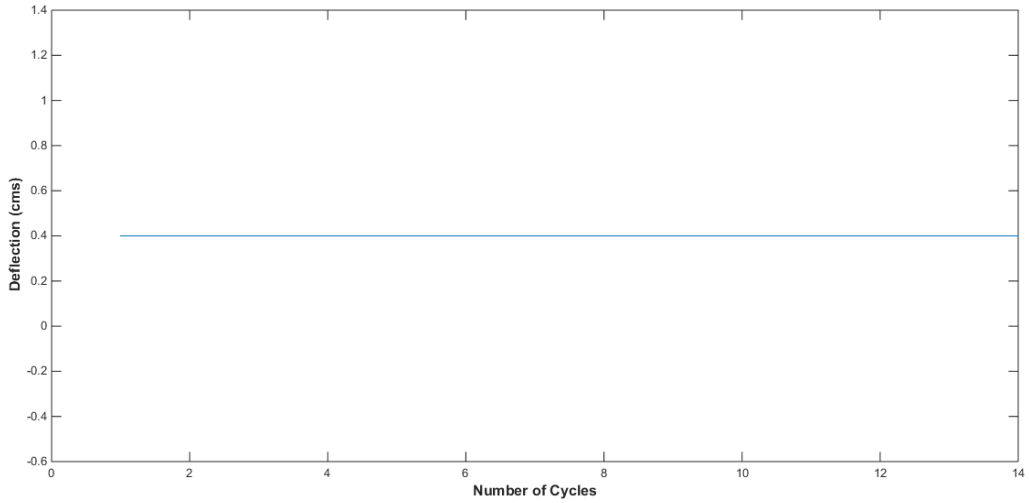

Figure 63 - Deflection Vs Number of Cycles for Latch Subsystem

2. Linear Actuation Mechanism

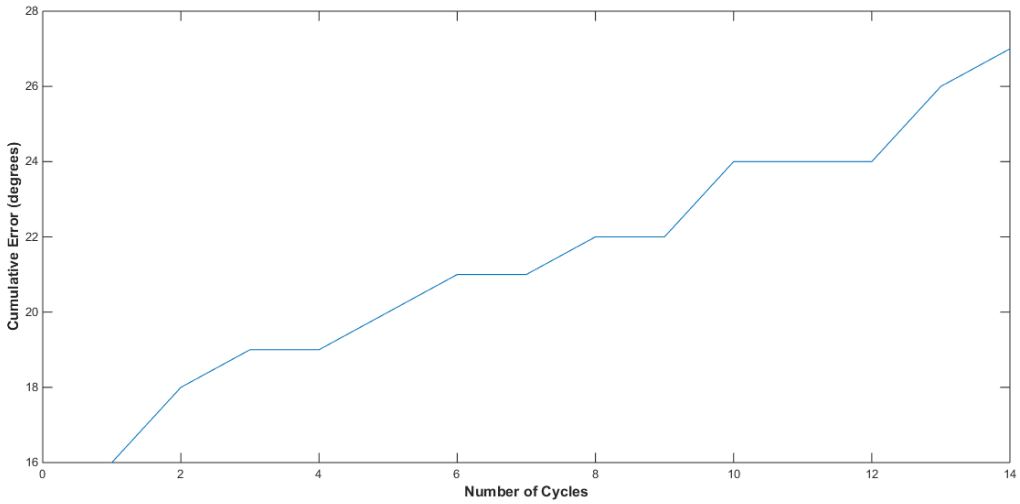

Figure 64 - Cumulative Error Vs Number of cycles for Linear Actuation Mechanism

From figure (63) and (64), it can be seen that the linear actuator has a greater effect on the precise working of the whole mechanism. This can be attributed to the fact that the deflection obtained by the latching mechanism is constant over a period of 14 cycles. However, the linear actuation mechanism has an increasing cumulative error curve over a period of 14 cycles. The reasons for this behavior of the linear actuator mechanism are similar to system level issues discussed above.

4.4 Performance Analysis

The systems mechanism involves linear movement of 3 actuators attached to the plane of the antenna and thus achieve a tip/tilt mechanism. The ability of the design for ±45 degree tip/tilt is limited currently due to the pivot angle of the ball and socket joint used in the mechanism to 20 degrees. To analyze the precise working of the system, the 3 actuators must perform identically. The linear movement of the 3 actuators was studied under the payload of a dummy antenna and the angles achieved were compared to determine the performance of each. The amount of time for which current was provided was varied in each case. The graphs obtained for each actuator are as shown –

For Actuator 1 –

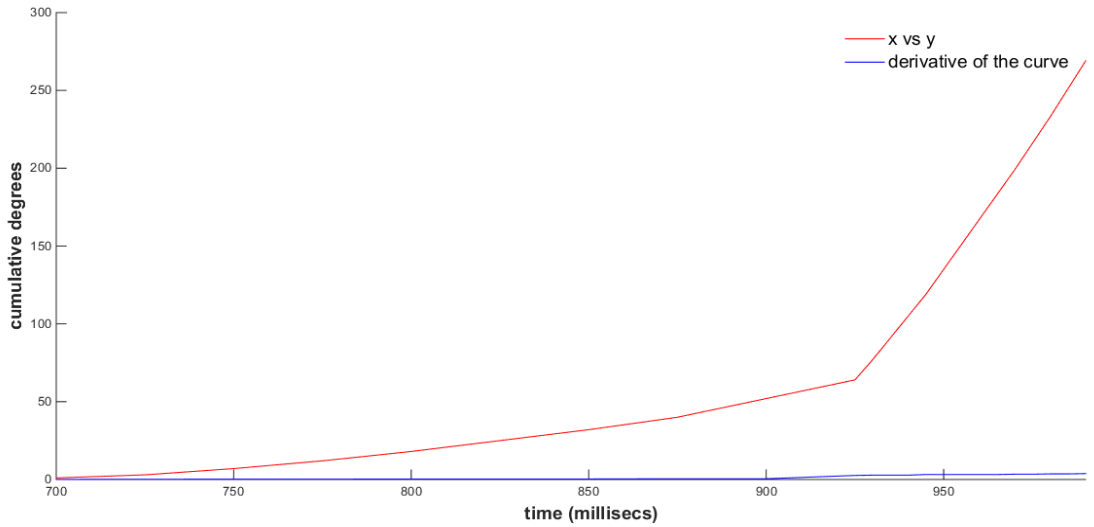

Figure 65 - Cumulative degrees achieved vs time for arm 1

For Actuator 2 -

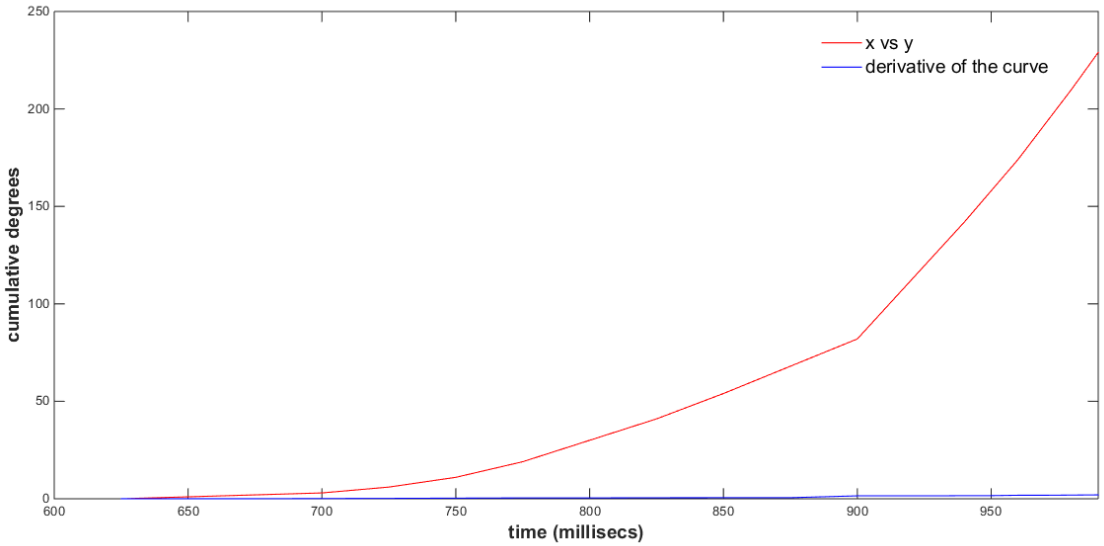

Figure 66 - Cumulative degrees achieved vs time for arm 2

For Actuator 3 -

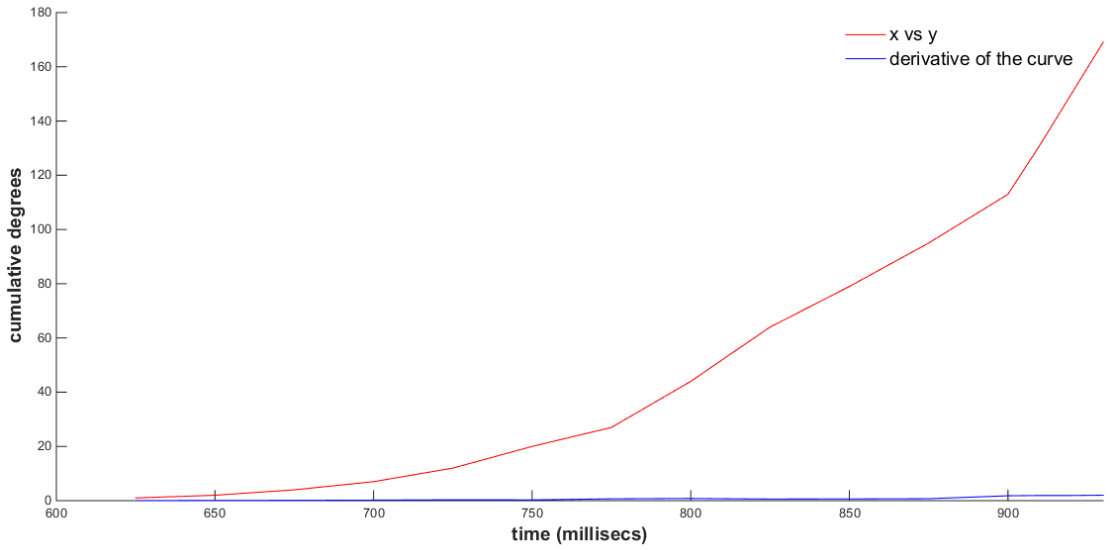

Figure 67 - Cumulative degrees achieved vs time for arm 3

From the trend obtained we can see that as the time for which the current is provided increases the contraction achieved also increases contributing to higher angle achieved. With lower time, the phase transformation of the total SMA wire structure is achieved partially, giving smaller contraction. In the final cycle, the current is sent for 1 sec, maximum permissible time not to overheat the wire, thus attaining maximum possible tilt of 20 degrees.

To study the rate at which the angle changes, we determined the 1st order derivative of all the curves, after using basic curve fitting tool in MATLAB. The results in all the 3 cases shows increasing slope line signifying increasing change in the angle achieved. Further significance can be observed by considering the derivative graph.

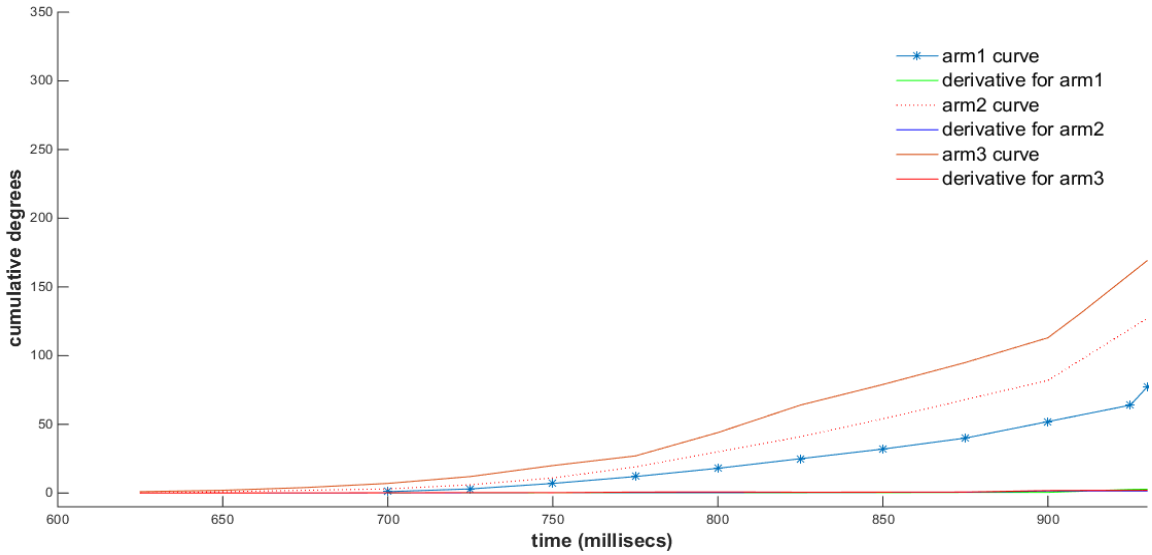

Figure 68 - Superimposed curve to show relative variation in error propagation for the 3 arms

Study of shape edges on the cumulative degree vs time graph –

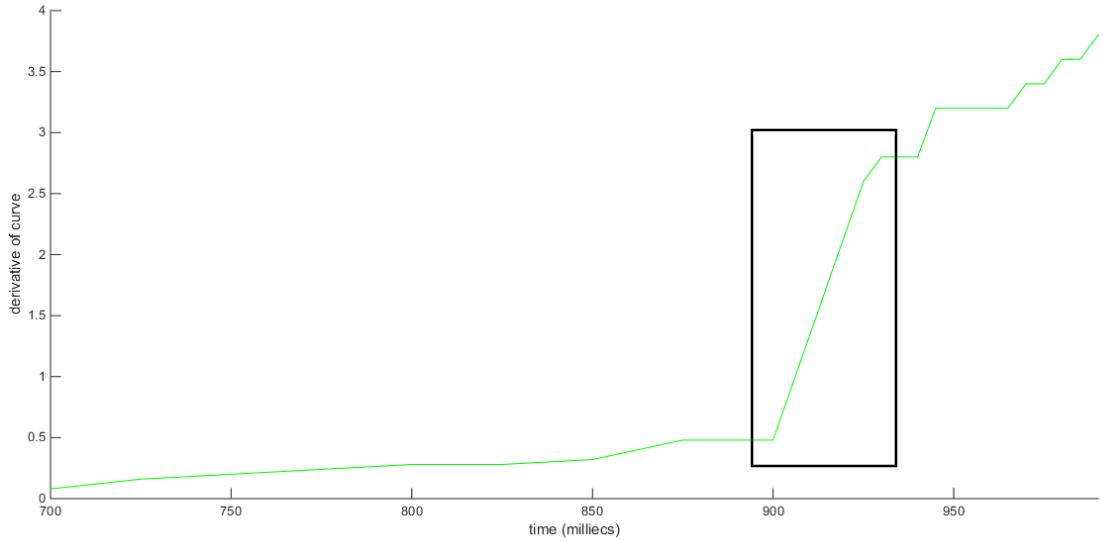

Figure 69 - Derivative study to see rate of change of angle of antenna

The study of the derivative shows a sudden rise in the curve slope, which is attributed to the fact that wire reaches the transition temperature range. The SMA wires work on the principle of Joules effect, and as time is varied the amount of heat generated increases. It

can be seen at around 900 milliseconds, the SMA wire reaches it transition temperature phase and thus shows sudden contraction in its size.

This is due to errors in setting up the assembly potential sources of errors are –

1. Placement of actuators

The actuators are placed in the form of an equilateral triangle with a fixed distance between their centers. Any error in manufacturing giving rise to uneven center to center distance might be a source of error.

2. Design Improvements –

The support plate for the vertical support structure, and also for the cylinder in which the ratcheted arms slide which was manufactured in discrete, if manufactured as 1 unit will mitigate the error intensity.

CHAPTER 5

MISSION CONCEPT

The present chapter describes a possible pathway to further develop the SMA pointing mechanism into a packaged space rated subsystem. The system design presented here is takes into account functional aspects of a space-worthy system such as low stowage volume and mass and relies on refinements in manufacturing methods to achieve tighter tolerances. Based on experimental understanding developed, we will discuss the feasibility of the design as a mission concept in the following sections.

5.1 Concept Definition

We propose using a stowed antenna pointing mechanism that occupies 1.3U in a 6U CubeSat. A 6U system was considered feasible as it leaves adequate room to house additional instrumentation to justify a science quality data mission. Figure with deployed antenna pointing mechanism.

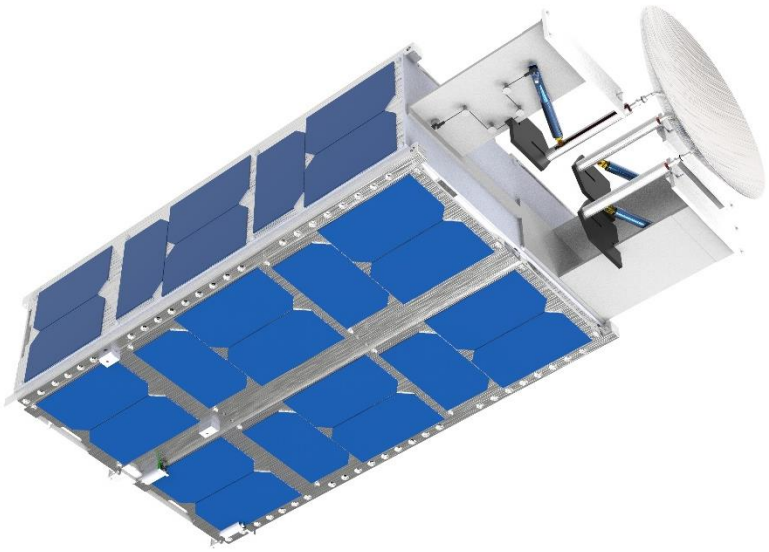

Figure 70 - Deployed APM on 6U CubeSat

5.2 System Overview

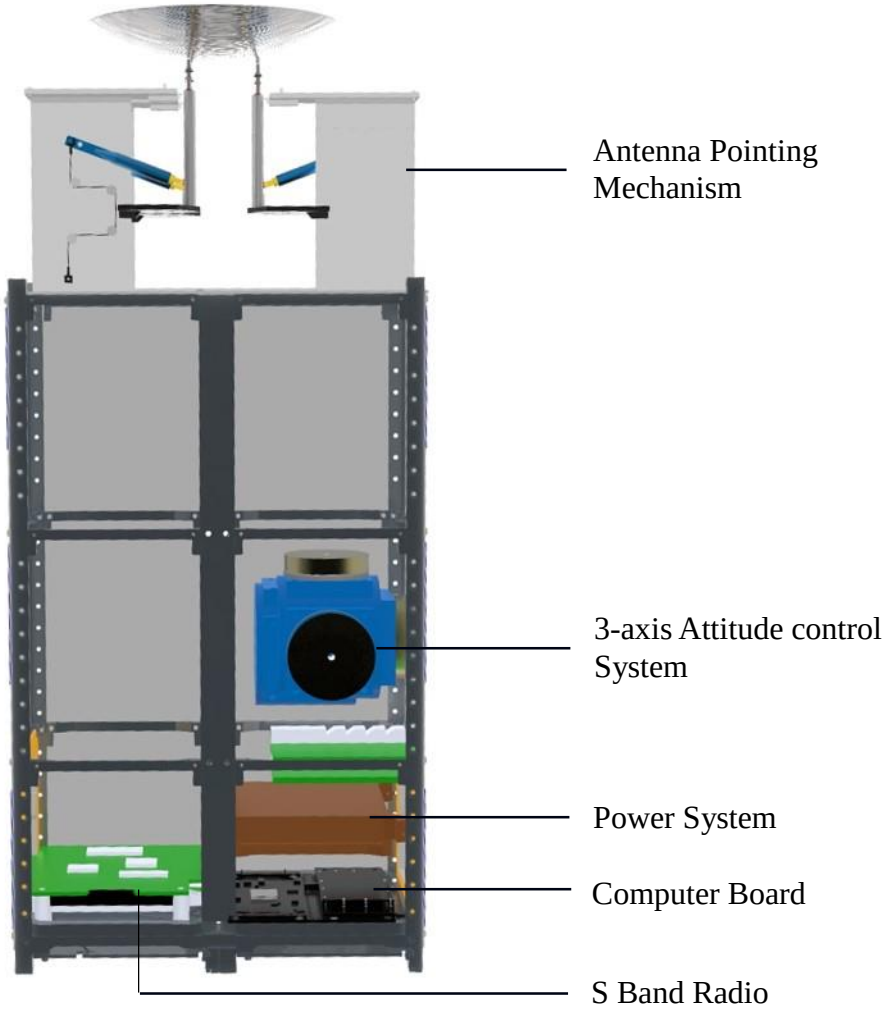

Figure 71 - System diagram with minimum required components

5.2.1 Antenna

The antenna pointing mechanism is designed to be used with any type of antenna. Presented is a parabolic dish type antenna. The dimensions for antenna shown in figure (71) are 15 cm Diameter, 3 cm Depth and having focal length as 7.031 cm.

5.2.2 Computer Board

The computer board proposed is a Tyvak controller with an arm 9 processor. This board has extensive heritage and has been optimized for Leo operations. Sensors like Inertial Measurement Unit (IMU), Star tracker, power sensor etc. are already integrated seamlessly on board. It also provides an architecture for additional external interfacing for Input/output control and image sensor integration. [31]

5.2.3 Radio (S band)

The S band radio communications have a pointing accuracy tolerance in the order of a few degrees [32]. The proposed antenna pointing mechanism is capable of providing 1°pointing based on calculations and experiments performed which meet the requirements imposed by the antenna beam width.

5.2.4 Battery (Power)+Solar panels

Re-chargeable Lithium ion batteries along with solar panel to charge them constitute the power system. The peak capacity of 15Whrs is offered by the batteries with the capacity to generate 120W/day for a normal instrument duty cycle. 30% is the efficiency of the solar panels.

5.2.5 ADCS(R wheels 3 axis)

CubeSat COTS (commercial off the shelf) products will be used as power source for the satellite as rechargeable battery units. It is proposed to use a 3-axis reaction wheel attitude control system. The control mechanism would also be responsible for perturbations introduced in the system due to rapid movement of the antenna while pointing applications. The tolerance for pointing accuracy is within 1° for S band radio communications.[32]

5.2.5 Verification System

The proposed verification system is based on displacement sensors. The vertical movement of the arms with respect to its initial position will be detected by the sensors which is returned as feedback as the angle displaced by the antenna. The desired angle command sent through the computer board sets the delay in latching based on values provided by the displacement sensors.

5.2.6 Mass and Volume Budget

The following table shows the mass and volume budget based on the proposed APM configuration –

Subsystem	**Unit**	**Mass (grams)**	**Maximum expected factor of error (%)**	**Maximum Mass (grams)**	**Volume (cm^3)**
Structure	System Chasis	2300	1.3	2990	188.64
Power System	Re-chargable batteries	100	1.3	130	37.81
Communication	Parabolic dish Antenna	21.2	1.1	23.32	
	Antenna pointing mechanism	3510	1	3510	1300
Attitude Control	Reaction wheels	345	1.1	379.5	180
Verification System	Displacement sensors	200	1	200	22.62
			average = 1.13	7232.82	1729.07

Table 4 - Mass and volume budget of proposed system

For a 6U satellite, the proposed configuration leaves 4200 cm^3 or 4.2U for scientific payloads.

Schematic diagram for the process of antenna pointing mechanism for a given command

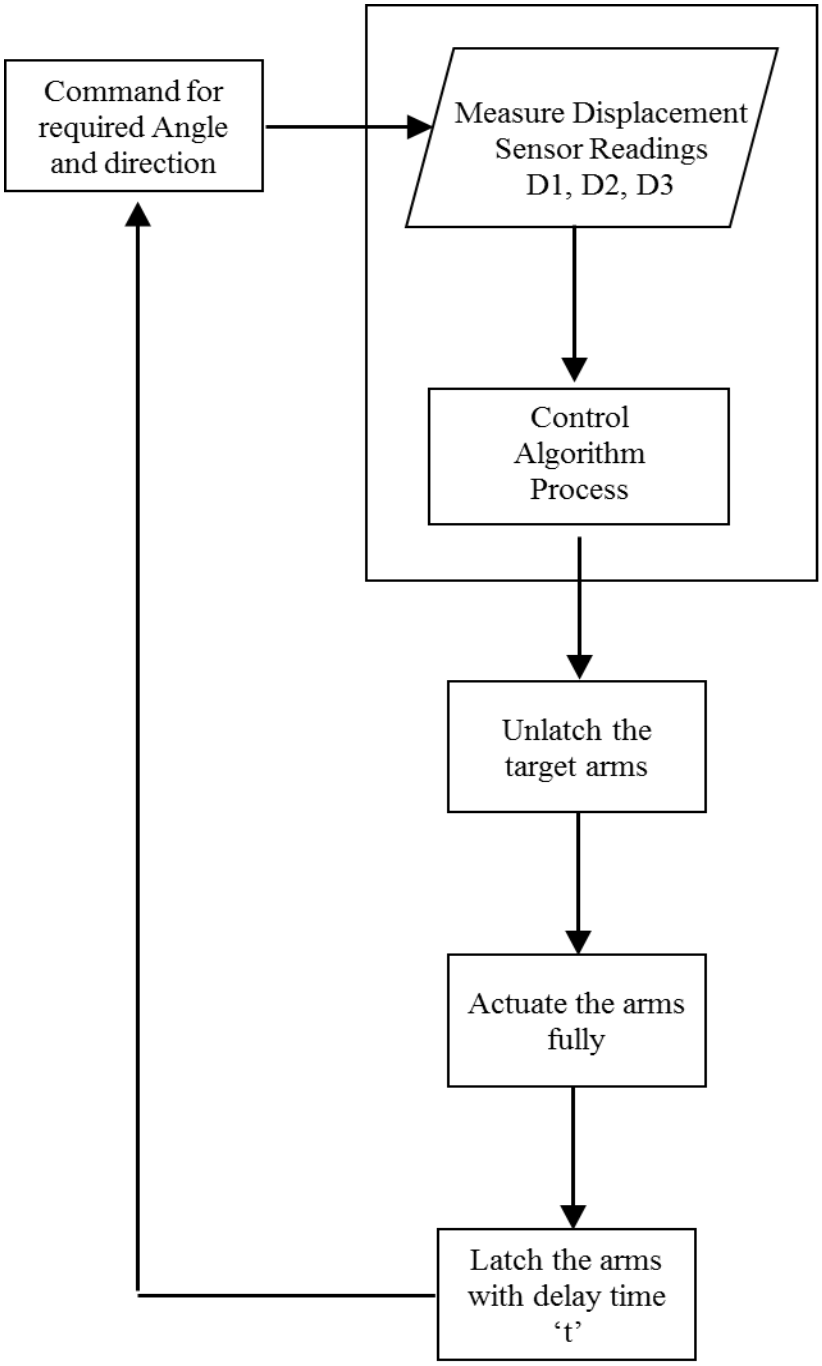

Figure 72 - Concept of Operation

CHAPTER 6

CONCLUSION

6.1 Conclusion

The ability of the SMA's for the application of large force and large stroke using simple mechanisms has been justified through this work. SMA used for proposed antenna pointing mechanism is unique in its application as from the literature survey the existing products don't have both the characteristics. The steps for angular tilt of 1 degree was achieved, and the experiments concluded the error propagation of 3 degrees cumulative over the range of 14 cycles.

Due to restriction based on the pivot angle of the ball and socket joint, the maximum angle which could be achieved was limited to 20 degrees. The system performance graphs helped verify the angular movement, along with minor differences in performance of each of the actuators due to design imperfections, manufacturing methods and temperature considerations.

The bench top model for the latching mechanism implemented proved to be successful with no degree of error considering its simplest design with minimal flaws or frictional losses. The liner actuation sub system along with latching mechanism forms the major sub systems of the antenna pointing mechanism. Error free latching, makes linear actuation system vulnerable to error, and can be proven from results with increasing cumulative error with increments in the number of cycles.

The major highlights of this section are -

1. The developed mechanism proves the feasibility of linear actuation of SMA's to be used for pointing mechanism of Antennas in space with steps of 1 degree and error of ±2 degrees cumulative.

2. The angle of tilt achievable from the experiments and calculations are verified to be same i.e. 20 degrees.

3. Lab scale demonstration of latching using SMA wires achieved without error in operation.

4. The error propagation in the linear actuation system due to manufacturing and design errors was observed leading to uncertainty in achieving precise control of APM.

6.2 Contributions:

1. SMA based Antenna pointing mechanism has been developed.

2. Angular tip/tilt of 45 degrees accurate to 1 degree has been achieved.

3. The mechanism can be applied to various payloads and is flexible in its construction depending on the application.

6.2 Future Work

1. Analysis and study of error propagation and effective actuation ability by using multiple wires to sustain varying gravity atmosphere effectively.
2. Development and Demonstration of active feedback control system.
3. Thermal modelling of the system and study of temperature profile for SMA's.
4. Studies and methods to achieve tip/tilt angle higher than 45°.

5. Modifications in design and use of precise manufacturing techniques for accuracy up to 0.1 degrees.

6. Design studies towards optimizing high strain SMA stowage for maximum packing efficiency.

7. Development of space worthy system.

REFERENCES

[1] Dunbar, Brian. NASA. 2004. Accessed November 15, 2016. https://www.nasa.gov/centers/langley/news/factsheets/Bldg-structures.html.

[2] "Adc.gsfc.nasa.gov." WebCompanyInfo.com - Information about Any Web Company. Accessed November 15, 2016. http://www.webcompanyinfo.com/adc.gsfc.nasa.gov.

[3] "Lunar Radio Telescope Project." TabView Example - Basic From Existing Markup. Accessed November 15, 2016. http://www.propagation.gatech.edu/ECE6390/project/Fall2006/Sharif/basic_from_markup.html.

[4] NASA. Accessed November 15, 2016. http://deepspace.jpl.nasa.gov/about/.

[5] By Mark E. Rosheim* and Gerald F. Sauter, Ph.D*. "Anthrobot.Com --- Ross-Hime Designs Inc." Anthrobot.Com --- Ross-Hime Designs Inc. Accessed October 29, 2016. http://www.anthrobot.com/press/article_new_omni_sensor_mount.php.

[6] Esa. "High Accuracy Position and Scanning Mechanisms." European Space Agency. Accessed October 29, 2016. http://www.esa.int/Our_Activities/Space_Engineering_Technology/Mechanisms/High_Accuracy_Position_and_Scanning_Mechanisms.

[7] Brunnen, A. J. D., and R. H. Bentall. 1982. Development of a high stability pointing mechanism for wide application.

[8] Bailly, Michel, and Eric Perez. "The pointing, acquisition and tracking system of Silex European program: a major technological step for intersatellites optical communication." In Proc. SPIE, vol. 1417, pp. 142-157. 1991.

[9] Inc., Moog. "Antenna Pointing Mechanisms." Antenna Pointing Mechanisms. Accessed October 29, 2016. http://www.moog.com/products/actuators-servoactuators/space/spacecraft/antenna-pointing-mechanisms.html.

[10] Bapna, Deepak, Eric Rollins, Alex Foessel, and Red Whittaker. "Antenna pointing for high bandwidth communications from mobile robots." In Robotics and Automation, 1998. Proceedings. 1998 IEEE International Conference on, vol. 4, pp. 3468-3473. IEEE, 1998.

[11] Ferris, Mark, and Nigel Phillips. "The use and advancement of an affordable, adaptable antenna pointing mechanism." In Proc. 14th Eur. Space Mech. Tribol. Symp, pp. 227-234. 2011.

[12] Goddard, N. D. R., R. M. J. Kemp, and R. Lane. "An overview of smart technology." *Packaging technology and science* 10, no. 3 (1997): 129-143.

[13] "Definition of a Shape Memory Alloy." Definition of a Shape Memory Alloy. Accessed November 03, 2016. http://smart.tamu.edu/overview/smaintro/simple/definition.html

[14] Huang, Weimin. "Shape memory alloys and their application to actuators for deployable structures." (1998).

[15] Butera, Francesco, Alberto Coda, Giorgio Vergani, and SAES Getters SpA. "Shape memory actuators for automotive applications." Nanotec IT newsletter. Roma: AIRI/nanotec IT (2007): 12-6.

[16] R., Santiago Anadón José. "Large Force Shape Memory Alloy Linear Actuator." PhD diss., 2002.

[17] Broquet, J., B. Claudinon, and A. Bousquet. 1985. Antenna pointing systems for large communications satellites. Journal of Guidance, Control, and Dynamics 8 (1): 71-7.

[18] Ferris, Mark, and Nigel Phillips. "The use and advancement of an affordable, adaptable antenna pointing mechanism." In *Proc. 14th Eur. Space Mech. Tribol. Symp*, pp. 227-234. 2011.

[19] "Gimbals & Pointing Mechanisms » NEA Electronics." Gimbals & Pointing Mechanisms » NEA Electronics. Accessed November 27, 2016. http://box.eba-d.com/products/gimbals-and-pointing-mechanisms/.

[20] "Technical Characteristics of Flexinol® Actuator Wires " Accessed October 29, 2016. http://dynalloy.com/pdfs/TCF1140.pdf.

[21] "Shape Memory Actuation - Corp.autosplice.com." Accessed November 3, 2016. http://corp.autosplice.com/App_Shared/Cache/100467/autosplice-shape-memory-actuators-brochure.pdf.

[22] “Dash4CutSheet - Miga Motors Online Store." Accessed October 29, 2016. http://www.migamotors.com/Media/Dash4CutSheet.pdf.

[23] Iwata, Toshiaki, Youichi Komoda, Akira Ogawa, and Hiroshi Murakami. "Solar paddle actuator for small satellites using shape memory alloy (II)." In 10th European Space Mechanisms and Tribology Symposium, vol. 524, pp. 409-412. 2003.

[24] Sreekumar, M., T. Nagarajan, and M. Singaperumal. 2009. Design of a shape memory alloy actuated compliant smart structure: Elastica approach. Journal of Mechanical Design, Transactions of the ASME 131 (6): 0610081-06100811.

[25] "Autosplice Inc. - Innovative Interconnections." Autosplice Inc. - Innovative Interconnections. Accessed October 29, 2016. http://www.autosplice-europe.com/.

[26] "TiNi Aerospace, Inc." TiNi Aerospace, Inc. Accessed October 29, 2016. http://www.tiniaerospace.com/ppconcept.html.

[27] Aerospace, TiNi. "Frangibolt." (2015). Harvard

[28] Gilberston, Roger G. Muscle wires project book. Edited by Celene De Miranda. Mondo. Tronics, 2000.

[29] "Outgassing.nasa.gov." Accessed November 3, 2016. http://outgassing.nasa.gov/cgi/uncgi/sectiona/sectiona.sh.

[30] "Constant Force Spring - Clock Springs - Spring Motor | Century Spring." Constant Force Spring - Clock Springs - Spring Motor | Century Spring. Accessed November 03, 2016. http://www.centuryspring.com/constant-force.

[31] "Tyvak." Tyvak. Accessed November 03, 2016. http://tyvak.eu/irm.html.

[32] Babuscia, Alessandra, B. Corbin, R. Jensen-Clem, M. Knapp, I. Sergeev, M. Van de Loo, and S. Seager. 2013. CommCube 1 and 2: A CubeSat series of missions to enhance communication capabilities for CubeSat.